



# Novel Biological Functions of the NsdC Transcription Factor in *Aspergillus fumigatus*

Patrícia Alves de Castro,<sup>a</sup> Clara Valero,<sup>a</sup> Jéssica Chiaratto,<sup>a</sup> Ana Cristina Colabardini,<sup>a,b</sup> Lakhansing Pardeshi,<sup>b,c</sup> Lilian Pereira Silva,<sup>a</sup>  Fausto Almeida,<sup>d</sup> Marina Campos Rocha,<sup>e</sup> Roberto Nascimento Silva,<sup>d</sup>  Iran Malavazi,<sup>e</sup> Wenyue Du,<sup>f</sup> Paul S. Dyer,<sup>f</sup> Matthias Brock,<sup>f</sup> Flávio Vieira Loures,<sup>g</sup> Koon Ho Wong,<sup>b,h</sup>  Gustavo H. Goldman<sup>a</sup>

<sup>a</sup>Faculdade de Ciências Farmacêuticas de Ribeirão Preto, Universidade de São Paulo, Ribeirão Preto, Brazil

<sup>b</sup>Faculty of Health Sciences, University of Macau, Taipa, Macau SAR, China

<sup>c</sup>Genomics and Bioinformatics Core, Faculty of Health Sciences, University of Macau, Taipa, Macau SAR, China

<sup>d</sup>Faculdade de Medicina de Ribeirão Preto, Universidade de São Paulo, Ribeirão Preto, Brazil

<sup>e</sup>Departamento de Genética e Evolução, Centro de Ciências Biológicas e da Saúde, Universidade Federal de São Carlos, São Carlos, São Paulo, Brazil

<sup>f</sup>Fungal Genetics and Biology Group, School of Life Sciences, University of Nottingham, Nottingham, United Kingdom

<sup>g</sup>Instituto de Ciência e Tecnologia, Universidade Federal de São Paulo, São José dos Campos, Brazil

<sup>h</sup>Institute of Translational Medicine, Faculty of Health Sciences, University of Macau, Taipa, Macau SAR, China

Patrícia Alves de Castro and Clara Valero contributed equally to this work. Author order was determined both alphabetically and in order of increasing seniority.

**ABSTRACT** The fungal zinc finger transcription factor NsdC is named after, and is best known for, its essential role in sexual reproduction (never in sexual development). In previous studies with *Aspergillus nidulans*, it was also shown to have roles in promotion of vegetative growth and suppression of asexual conidiation. In this study, the function of the *nsdC* homologue in the opportunistic human pathogen *A. fumigatus* was investigated. NsdC was again found to be essential for sexual development, with deletion of the *nsdC* gene in both *MAT1-1* and *MAT1-2* mating partners of a cross leading to complete loss of fertility. However, a functional copy of *nsdC* in one mating partner was sufficient to allow sexual reproduction. Deletion of *nsdC* also led to decreased vegetative growth and allowed conidiation in liquid cultures, again consistent with previous findings. However, NsdC in *A. fumigatus* was shown to have additional biological functions including response to calcium stress, correct organization of cell wall structure, and response to the cell wall stressors. Furthermore, virulence and host immune recognition were affected. Gene expression studies involving chromatin immunoprecipitation (ChIP) of RNA polymerase II (PolIII) coupled to next-generation sequencing (Seq) revealed that deletion of *nsdC* resulted in changes in expression of over 620 genes under basal growth conditions. This demonstrated that this transcription factor mediates the activity of a wide variety of signaling and metabolic pathways and indicates that despite the naming of the gene, the promotion of sexual reproduction is just one among multiple roles of NsdC.

**IMPORTANCE** *Aspergillus fumigatus* is an opportunistic human fungal pathogen and the main causal agent of invasive aspergillosis, a life-threatening infection especially in immunocompromised patients. *A. fumigatus* can undergo both asexual and sexual reproductive cycles, and the regulation of both cycles involves several genes and pathways. Here, we have characterized one of these genetic determinants, the NsdC transcription factor, which was initially identified in a screen of transcription factor null mutants showing sensitivity when exposed to high concentrations of calcium. In addition to its known essential roles in sexual reproduction and control of growth rate and asexual reproduction, we have shown in the present study that *A. fumigatus* NsdC transcription factor has additional previously unrecognized biological functions including calcium tolerance, cell wall stress response, and correct cell wall organization and

**Citation** Alves de Castro P, Valero C, Chiaratto J, Colabardini AC, Pardeshi L, Pereira Silva L, Almeida F, Campos Rocha M, Nascimento Silva R, Malavazi I, Du W, Dyer PS, Brock M, Vieira Loures F, Wong KH, Goldman GH. 2021. Novel biological functions of the NsdC transcription factor in *Aspergillus fumigatus*. *mBio* 12:e03102-20. <https://doi.org/10.1128/mBio.03102-20>.

**Editor** J. Andrew Alspaugh, Duke University Medical Center

**Copyright** © 2021 Alves de Castro et al. This is an open-access article distributed under the terms of the [Creative Commons Attribution 4.0 International license](https://creativecommons.org/licenses/by/4.0/).

Address correspondence to Gustavo H. Goldman, [ggoldman@usp.br](mailto:ggoldman@usp.br).

**Received** 2 November 2020

**Accepted** 9 November 2020

**Published** 5 January 2021

functions in virulence and host immune recognition. Our results indicate that NsdC can play novel additional biological functions not directly related to its role played during sexual and asexual processes.

**KEYWORDS** *Aspergillus fumigatus*, sexual cycle, transcription factor, cell wall integrity pathway, calcium signaling, transcription factors

**A** *Aspergillus fumigatus* is an opportunistic human fungal pathogen and the main causal agent of invasive aspergillosis, a life-threatening infection especially in immunocompromised patients (1). It is estimated that 300,000 infections occur per year worldwide with an associated mortality that could reach 95% (2, 3). The fungus is ubiquitous in the environment, and the infection is acquired mainly by inhalation of conidia present in the air (4). These conidia are produced on structures called conidiophores which are characteristic of asexual reproduction in *Aspergillus* species (5, 6). *A. fumigatus* can undergo both asexual and sexual reproductive cycles, but whereas asexual reproduction is observed in almost all aspergilli, sexual reproduction has been detected only in approximately 36% of *Aspergillus* species (7, 8).

The regulation of asexual reproduction involves several genes and pathways in *A. fumigatus*. A highly conserved pathway has been described as the central regulatory mechanism of asexual development in *Aspergillus* species such as *A. fumigatus* (6). It involves three key regulators that behave as a cascade activating each other in sequential order: BrlA, a transcription factor (TF) which is an essential activator; AbaA, responsible for hyphal differentiation into phialides; and WetA, important for conidial maturation (9–13). Accumulation of mRNA of the *abaA* and *wetA* genes was detected during asexual reproduction of *A. fumigatus*, while deletion of *brlA* impaired *abaA* and *wetA* transcript production (12). Further complementary regulatory mechanisms have also been reported to play a role in the genetic control of conidiation, such as the velvet family of negative regulator proteins (14), the FluG and FlbA-E upstream activators (11, 15), and members of the heterotrimeric G-protein signaling pathway (6, 11, 16, 17). Moreover, we have recently found that the mitogen-activated protein kinase MpkB is also important for conidiation and melanin production in *A. fumigatus* (18).

Despite evidence for cryptic sexual development in *A. fumigatus* having already been reported in the literature (19–21), it was not until 2009 that O’Gorman and colleagues were able to demonstrate the induction of a heterothallic (obligate outbreeding) sexual cycle under well-defined laboratory conditions (22). This involved formation of sexual fruiting bodies known as cleistothecia which at maturity contained sexual ascospores, with evidence provided for genetic recombination in the offspring. Sexual reproduction was found to require very specific environmental conditions not easily found in nature and incubation for up to 12 months. However, the subsequent identification of “supermater” strains (with enhanced sexual fertility) has facilitated the investigation of this process in a laboratory setting (23). The sexual cycle has provided an excellent tool not just for expanding basic genetic studies but also for investigating and explaining medically important processes such as the acquisition of azole resistance or differences in virulence in strains of *A. fumigatus* (24). The breeding system in *A. fumigatus* is governed by the presence of two mating-type (*MAT*) genes (*MAT1-1* and *MAT1-2*) which encode alpha- and high-mobility group (HMG) domain transcription factors, respectively, and determine sexual identity of isolates (6, 20). Deletion of either of these genes resulted in a block in cleistothecium formation (25). Distribution of the compatible mating types has been reported to be near 1:1 in both regional and global populations of the fungus (20, 26).

Although a sexual cycle has only recently been described in *A. fumigatus*, *Aspergillus nidulans* has long been established as a model organism for studying processes controlling sexual development in ascomycete fungi. Beyond *MAT* genes, a wide list of over 70 sex-related genes has also been identified in *A. nidulans*, including genes with roles in light

and nutrient sensing, signal transduction pathways, genes encoding transcription factors and other regulatory proteins, or even genes linked to endogenous physiological processes (27). Some of these findings have been confirmed to apply to *A. fumigatus*, such as the involvement of the transcription factor NsdD in hyphal fusion, necessary for heterokaryon formation (25). However, it is important to note that whereas *A. fumigatus* is a heterothallic species, in contrast *A. nidulans* is a homothallic (self-fertile) species and there is limited evidence that the regulation of sexual reproduction may differ slightly in homothallic versus heterothallic species (28).

The NsdC (never in sexual development) transcription factor was first identified in *A. nidulans* specifically due to its requirement for sexual reproduction. It encodes a fungus-specific C<sub>2</sub>H<sub>2</sub>-type zinc finger transcription factor, and its loss resulted in the lack of fruiting body formation, retarded vegetative growth, and hyperactive asexual sporulation (29). In the present work, we have characterized the homologous NsdC transcription factor from *A. fumigatus*, which was initially identified in a screen of transcription factor null mutants showing sensitivity when exposed to high concentrations of calcium (30). Besides calcium, we now report that the  $\Delta nsdC$  strain exhibits increased sensitivity to cell wall-damaging agents. Furthermore, deletion of *nsdC* in both mating partners was found to completely abolish sexual development, while asexual conidiation was derepressed in liquid medium. Transmission electron microscopy, cell wall staining studies, and cell wall sugar content measurements showed that NsdC is involved in cell wall organization and composition, while genome-wide transcription profiling analysis (as measured by RNA polymerase II [PolII] occupancy) revealed NsdC has roles in several important biological responses. Finally, the  $\Delta nsdC$  strain displayed a reduction in mortality and fungal burden in a neutropenic mouse model of invasive aspergillosis coupled with enhanced killing by macrophages. In summary, it is concluded that NsdC is important not only for sexual and asexual development but also for calcium tolerance and cell wall damage stress response by affecting cell wall composition and organization and has a role in virulence of *A. fumigatus*.

## RESULTS

**NsdC is important for calcium tolerance.** We previously identified, in a library of 395 *A. fumigatus* TF null mutants, nine null mutants that exhibited increased sensitivity to 500 mM calcium chloride (30). Among these TF mutants, we observed  $\Delta nsdC$  (Afu7g03910), a putative homologue of *A. nidulans* NsdC (AN4263), a C<sub>2</sub>H<sub>2</sub> zinc finger TF required for sexual development (29). In order to investigate the function of *nsdC* in *A. fumigatus*, the null mutant strain was here complemented by reinsertion of the wild-type gene and aspects of growth were compared between the deletion mutant and the complemented strain. The deletion of *nsdC* in *A. fumigatus* affected about 30 and 10% radial growth reduction on solid minimal medium (MM) and complete medium (yeast agar glucose [YAG]), respectively (Fig. 1A). There is about 20% growth reduction in liquid MM in 24-h growth compared to the wild type, but at 48 h growth is comparable to both wild-type and complemented strains (Fig. 1A, right panel). Interestingly, there are no growth differences in liquid YG medium for all three strains (Fig. 1A, right panel). The  $\Delta nsdC$  mutant was more sensitive to calcium (CaCl<sub>2</sub>) (Fig. 1B) and exhibited enhanced resistance to the calcineurin activity inhibitor cyclosporine (Fig. 1C). We included these experiments with cyclosporine to see the relationship between calcineurin and NsdC. The  $\Delta calA$  mutant (null mutant for the calcineurin catalytic subunit) is also sensitive to calcium but resistant to cyclosporine (Fig. 1B and C). The  $\Delta crzA$  mutant is sensitive to calcium but as sensitive to cyclosporine as the wild-type strain (Fig. 1B and C). We have not observed differences between the morphology and growth of the wild-type and  $\Delta nsdC$  germlings (Fig. 1D). NsdC-GFP (green fluorescent protein) under the control of the *nsdC* promoter (the cassette was homologously integrated in the *nsdC* locus) was constitutively present in the nucleus, and there was no clear effect on its translocation to the cytoplasm and/or degradation after exposure to high concentrations of CaCl<sub>2</sub> or

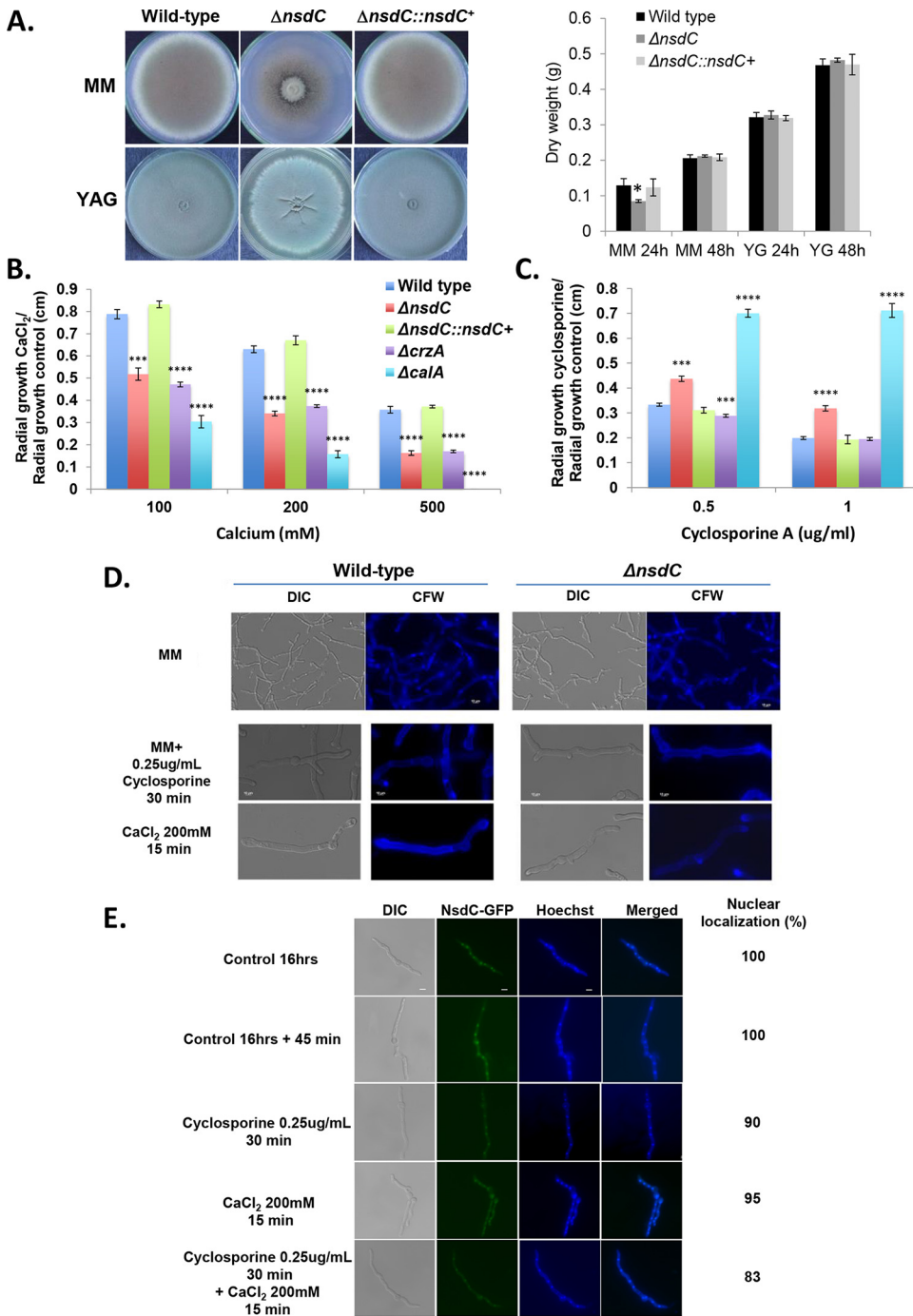


**FIG 1** Growth phenotypes for  $\Delta nsdC$ . (A to C) The wild-type,  $\Delta nsdC$ , and  $\Delta nsdC::nsdC^+$  strains were grown for 5 days on solid MM and YAG or for 2 days in liquid MM and YG at 37°C (A), MM +  $CaCl_2$  (B), and MM + cyclosporine (C). Results are expressed as radial growth of treatment/radial growth of control (centimeters) and are the average of three independent biological repetitions  $\pm$  standard deviation. The statistical analysis was one-tailed, paired *t* test. *P* values: \*, *P* < 0.05; \*\*, *P* < 0.01; \*\*\*, *P* < 0.001; \*\*\*\*, *P* < 0.0001. (D) Conidia of the wild-type and  $\Delta nsdC$  strains were germinated for 16 h at 37°C in liquid MM and exposed or not to 0.25  $\mu$ g/ml cyclosporine for 30 min or 200 mM  $CaCl_2$  for 15 min. Germlings were stained with calcofluor white (CFW). DIC, differential interference contrast. First row shows  $\times 40$  magnification while second and third rows show  $\times 100$  magnification. (E) NsdC-GFP germlings were grown for 16 h at 37°C in MM and exposed to 200 mM  $CaCl_2$  for 15 min or 0.25  $\mu$ g/ml cyclosporine for 30 min followed by 200 mM  $CaCl_2$  for 15 min. About 100 germlings were counted in each treatment. Bar, 5  $\mu$ m. Statistical analysis was performed using a one-way ANOVA comparing both  $\Delta nsdC$  and  $\Delta nsdC::nsdC^+$  strains to the wild type (\*\*\*\*, *P* < 0.0001).

cyclosporine (Fig. 1E). Taken together, these results strongly suggest that NsdC is involved in the *A. fumigatus* calcium response pathway.

**Generation of  $\Delta nsdC$  mutants in high-fertility *MAT1-1* and *MAT1-2* mating-type backgrounds.** In the homothallic fungus *Aspergillus nidulans*, the *nsdC* gene is crucial for sexual development (29). Therefore, it was of interest to investigate whether the same is true for the heterothallic fungus *A. fumigatus*. Unfortunately, the *MAT1-1* wild-type strain CEA17 (and its KU<sup>80</sup> mutant and derivatives used elsewhere in the present study) was found to be sterile in preliminary crossing efforts, which made it difficult to assess the specific contribution of *nsdC* to sexual development in this background. To overcome this limitation, the *nsdC* gene was instead deleted in the high-fertility *MAT1-1* wild-type strain 47-51 (AfIR974 [22]). As expected, some of the transformants displayed a condensed growth phenotype and green pigmentation of the mycelium on the regeneration plates, consistent with the phenotype observed with the  $\Delta nsdC$  mutation in the CEA17 background (Fig. 1A), and *nsdC* deletion was confirmed in these transformants.

To test the fertility of  $\Delta nsdC$  mutants with the 47-51 parental background, and to potentially generate  $\Delta nsdC$  mutants with a *MAT1-2* mating-type background, crosses were set up between the known fertile *A. fumigatus* *MAT1-2* strains 47-55 and 47-107 and two representative  $\Delta nsdC$  *MAT1-1* mutants, 47-51 $\Delta nsdC4$  and 47-51 $\Delta nsdC5$  (see Table S1 at <https://doi.org/10.6084/m9.figshare.12931754.v3>). All crosses were found to produce cleistothecia and viable ascospores (see Table S2 at <https://doi.org/10.6084/m9.figshare.12931754.v3>). This clearly demonstrated that *nsdC* is not essential for fertility in crosses with a heterothallic wild-type mating partner, at least when *nsdC* is deleted in the *MAT1-1* genetic background. The  $\Delta nsdC$  mutants appeared to show slightly lower fertility than the 47-51 parent when crossed to isolate 47-55, but this reduction was not statistically significant ( $F = 1.369$ ;  $P$  value = 0.2820). When ascospores were plated on a medium without pyrithiamine, both wild-type and  $\Delta nsdC$  mutant phenotypes were observed, whereas only the  $\Delta nsdC$  phenotype occurred on plates with pyrithiamine (Fig. 2A to D). This was consistent with the use of the pyrithiamine resistance cassette in *nsdC* deletion. Ascospore offspring from crosses between 47-51 $\Delta nsdC5$  and 47-107 and between 47-51 $\Delta nsdC5$  and 47-55 were then randomly selected from the pyrithiamine plate and analyzed for their mating type (Fig. 2A to D). These  $\Delta nsdC$  progeny showed an approximate 1:1 ratio of *MAT1-1* to *MAT1-2* genotypes, confirming that sexual recombination had occurred as demonstrated by the appearance of the novel  $\Delta nsdC$  *MAT1-2* genotypes (Fig. 2A to D; see also Table S1 at <https://doi.org/10.6084/m9.figshare.12931754.v3>).

PCR analysis of these transformants further confirmed the successful modification of the *nsdC* gene in these transformants (see Fig. S1 at <https://doi.org/10.6084/m9.figshare.12931754.v3>).

**Impact of both *MAT1-1* and *MAT1-2* *nsdC* deletion on sexual crossing of *A. fumigatus*.** Since a *MAT1-1*  $\Delta nsdC$  strain was fertile when crossed with a highly fertile *MAT1-2* strain, we were interested to see whether this also held true for a  $\Delta nsdC$  mutant with a *MAT1-2* mating-type background. Furthermore, we investigated the result of crossing of eight additional  $\Delta nsdC$  strains, comprised of two *MAT1-1* and two *MAT1-2* strains from progeny of each of crosses between 47-51- $\Delta nsdC5$  and 47-55 or 47-51- $\Delta nsdC5$  and 47-107 (see Table S2 at <https://doi.org/10.6084/m9.figshare.12931754.v3>).

As shown in Table 1 and Fig. 2E to H, cleistothecia were formed in all control crosses between *MAT1-1* and *MAT1-2* wild-type isolates, and also in almost all crosses when at least one mating partner contained a functional copy of the *nsdC* gene, irrespective of whether it was a *MAT1-1* or *MAT1-2* partner that contained the functional copy. The only exceptions were crosses 47-267  $\times$   $\Delta nsdC-w$  and 47-107  $\times$   $\Delta nsdC-y$ , which failed to form cleistothecia, but importantly strains  $\Delta nsdC-w$  and  $\Delta nsdC-y$  formed cleistothecia with the alternative mating partners 47-51 and 47-55, respectively. In contrast, deletion of *nsdC* in both mating partners resulted in a complete lack of the formation of cleistothecia in all 16 test crosses, despite incubation for an extended period of 6 months and the formation of a barrage zone between the partners (Table 1; Fig. 2E to H). Therefore, it can be concluded that whereas gene activation by *nsdC* in one mating

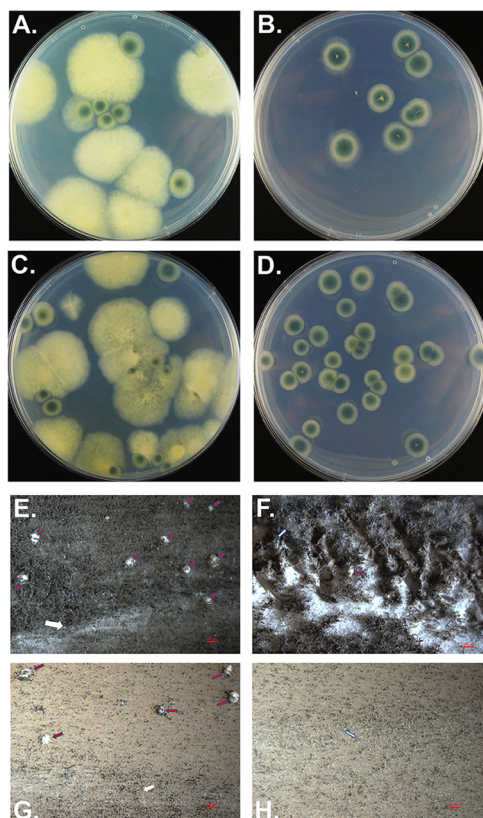


**FIG 2** Sexual crosses of the  $\Delta nsdC$  mutant. Appearance of sexual progeny from crosses using 47-51 $\Delta nsdC$  (5) as a mating partner, in which *nsdC* was deleted by replacement with a pyrithiamine resistance cassette. (A and B) Offspring of the cross 47-51 $\Delta nsdC$  (5)  $\times$  47-55. (C and D) Offspring of the cross 47-51  $\Delta nsdC$  (5)  $\times$  47-107. Ascospore progeny were spread plated onto either Glucose 50, Gln 10 (A and C) or Glucose 50, Gln 10, PT (pyrithiamine) 0.1 (B and D) medium; see Materials and Methods for details. All pyrithiamine-resistant (at 0.1  $\mu\text{g/ml}$  PT) offspring (B and C) show the  $\Delta nsdC$  phenotype. (E to H) Cleistothecia formed by representative mating partners of *A. fumigatus* on oatmeal agar following incubation for 4 months in darkness at 30°C. Images photographed after “hoovering” of plates as appropriate to allow clearer visualization of cleistothecia. Red arrows indicate cleistothecia, and white arrows indicate the barrage zone where two mating types of *A. fumigatus* strains met. Bar, 500  $\mu\text{m}$ . (E) Cleistothecia formed in a cross between strains 47-267 (*MAT1-1*) and 47-55 (*MAT1-2*). (F) Cleistothecia formed in a cross between 47-267 and  $\Delta nsdC$ -a (*MAT1-2*). (G) Cleistothecia formed by 47-55 and  $\Delta nsdC$ -b (*MAT1-1*). (H) Absence of cleistothecia in a cross between  $\Delta nsdC$ -a and  $\Delta nsdC$ -b.

partner is sufficient to initiate and allow completion of the sexual cycle, the absence of *nsdC* in both mating partners instead totally abolishes sexual development.

**NsdC is involved in the control of asexual sporulation.** The  $\Delta nsdC$  strain displayed deregulation in initiation of conidiation in liquid MM, with conidiophores and conidia being produced, unlike the control wild-type parent and complemented strains

**TABLE 1** Formation of cleistothecia in crosses between various *MAT1-1 A. fumigatus* wild-type and  $\Delta nsdC$  strains and various *MAT1-2 A. fumigatus* wild-type and  $\Delta nsdC$  strains<sup>a</sup>

| <i>MAT1-2 strain</i> | <i>MAT1-1 strain</i> |                |                  |                  |                  |                  |
|----------------------|----------------------|----------------|------------------|------------------|------------------|------------------|
|                      | 47-51                | 47-267         | $\Delta nsdC$ -b | $\Delta nsdC$ -z | $\Delta nsdC$ -y | $\Delta nsdC$ -d |
| 47-55                | 7.0 $\pm$ 5.7        | 29.7 $\pm$ 8.0 | 13.8 $\pm$ 9.2   | 2.8 $\pm$ 2.1    | 7.8 $\pm$ 7.6    | 8.3 $\pm$ 11.0   |
| 47-107               | 14.2 $\pm$ 8.7       | 0.3 $\pm$ 0.5  | 4.0 $\pm$ 4.7    | 0.5 $\pm$ 0.6    | 0                | 0.5 $\pm$ 1.0    |
| $\Delta nsdC$ -a     | 0.5 $\pm$ 1.0        | 1.5 $\pm$ 1.7  | 0                | 0                | 0                | 0                |
| $\Delta nsdC$ -c     | 5.5 $\pm$ 5.9        | 2.7 $\pm$ 5.5  | 0                | 0                | 0                | 0                |
| $\Delta nsdC$ -x     | 35.0 $\pm$ 21.8      | 21.2 $\pm$ 8.1 | 0                | 0                | 0                | 0                |
| $\Delta nsdC$ -w     | 40.7 $\pm$ 18.9      | 0              | 0                | 0                | 0                | 0                |

<sup>a</sup>Numbers indicate average numbers of cleistothecia per 9-cm crossing plate  $\pm$  SEM.

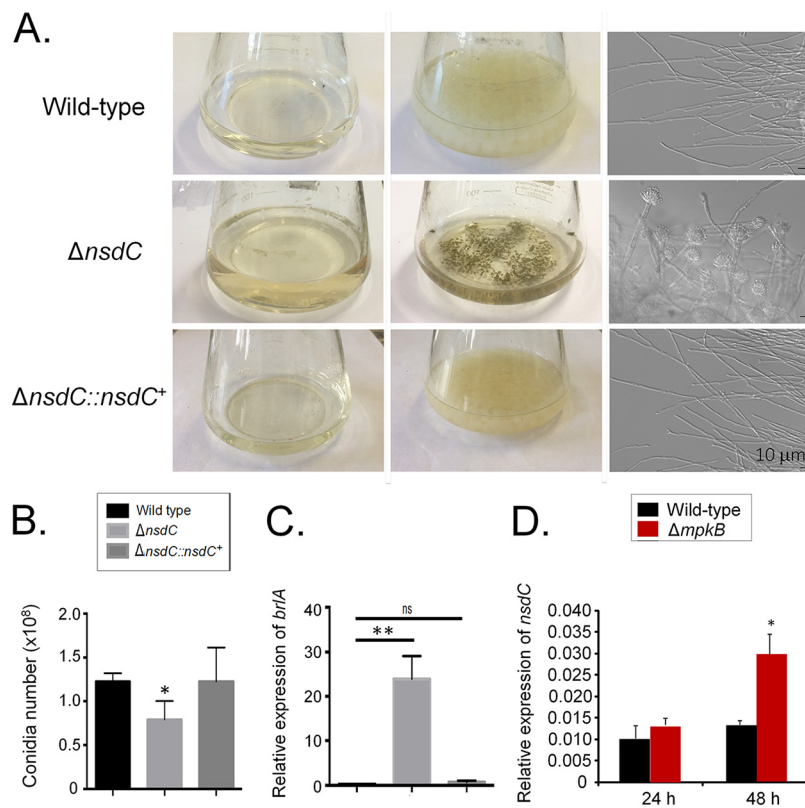


**FIG 3** The *A. fumigatus nsdC* null mutant produces conidiophores in liquid cultures with agitation. (A) Cultures (center column) and separated supernatants from the same cultures (left column) were grown with agitation for 5 days at 37°C. DIC microscopic analysis revealed the presence of conidia and conidiophores in the  $\Delta nsdC$  cultures (right column). (B) Number of conidia in the wild-type,  $\Delta nsdC$ , and  $\Delta nsdC::nsdC^+$  strains grown for 5 days at 37°C on MM. (C) The wild-type,  $\Delta nsdC$ , and  $\Delta nsdC::nsdC^+$  strains were grown for 24 h at 37°C in MM. Gene expression was obtained for *brlA* and was normalized by using *tubA* (Afu1g10910). (D) The wild-type and  $\Delta mpkB$  strains were grown for 24 or 48 h at 37°C in MM. Gene expression was obtained for *nsdC* and was normalized by using *tubA* (Afu1g10910). Error bars represent standard deviations of the average of three independent biological repetitions (each with 2 technical repetitions). Statistical analysis was performed using a one-way ANOVA compared to the wild-type condition (\*,  $P < 0.05$ ; \*\*,  $P < 0.01$ ; ns, not significant).

(Fig. 3A). However, a significant reduction in the number of conidia produced on solid MM by the  $\Delta nsdC$  strain was observed in comparison to the control strains (Fig. 3B). Previous reports described that the transcription factor BrlA is important for the activation of conidial development in *A. fumigatus* (11). RT-qPCR experiments showed that *brlA* expression in the  $\Delta nsdC$  strain was 25 times higher in liquid MM than in the wild-type and complemented strains (Fig. 3C). We have previously observed that the mitogen-activated protein (MAP) kinase MpkB plays an important role in the negative control of conidiation in liquid medium (18). The accumulation of *nsdC* mRNA was dependent on MpkB since there was a 2-fold increase in the *nsdC* mRNA transcripts in the  $\Delta mpkB$  strain compared with the wild-type strain after 48-h growth in liquid medium (Fig. 3D). These results indicate that NsdC is involved in suppression of conidiation in liquid culture but also has a role in promoting hyphal vegetative growth and concomitant asexual sporulation on solid media (as per Fig. 1A) and that *nsdC* expression is, at least to some degree, dependent on MpkB.

**NsdC participates in organization of the cell wall.** Although 1.2 M sorbitol improved  $\Delta nsdC$  mutant radial growth (Fig. 4A), the mutant strain was more sensitive to the chitin synthase inhibitor nikkomycin Z (Fig. 4B) and other cell wall-damaging agents, including Congo red (CR), calcofluor white (CFW), and caspofungin than were the wild-type and complemented strains (Fig. 4C to E). Increased sensitivity to cell wall stressors suggested the  $\Delta nsdC$  mutant had an altered cell wall composition. Cell wall

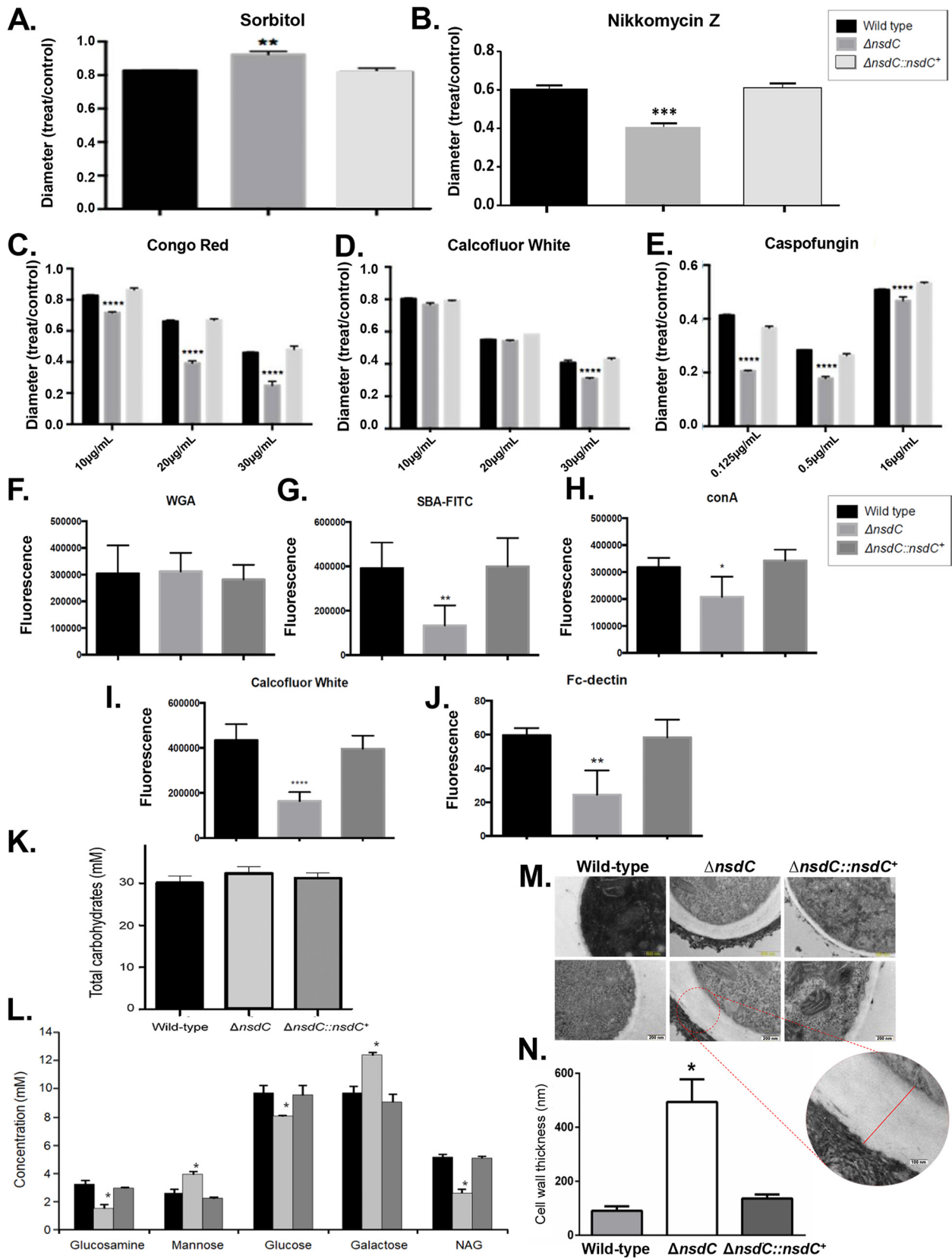


**FIG 4** *A. fumigatus* NsdC affects the cell wall organization and structure. (A to E) The wild-type,  $\Delta nsdC$ , and  $\Delta nsdC::nsdC^+$  strains were grown for 5 days at 37°C in MM + sorbitol at 1.2 M (A), MM + nikkomycin Z at 100 $\mu$ M (B), MM + Congo red up to 30 $\mu$ g/ml (C), MM + calcofluor white up to 30 $\mu$ g/ml (D), and MM + caspofungin up to 16 $\mu$ g/ml (E). Error bars represent standard deviations of the average of three (Continued on next page)

stains and fluorescently labeled lectins were therefore used to identify differences in the ability to detect (i.e., exposure of) several carbohydrates on the cell wall surface, for the wild-type,  $\Delta nsdC$ , and complemented strains. These included (i) WGA (wheat germ agglutinin)-FITC (fluorescein isothiocyanate), recognizing surface-exposed glucosamine (Glc); (ii) SBA (soybean agglutinin)-FITC, which binds preferentially to oligosaccharide structures with terminal  $\alpha$ - or  $\beta$ -linked *N*-acetylgalactosamine (GalNAc) and to galactose residues which are important for recognizing galactosaminogalactan (GAG); (iii) ConA (concanavalin A)-FITC, which recognizes  $\alpha$ -linked mannose; (iv) CFW (recognizing chitin); and (v) soluble dectin-1 staining (recognizing  $\beta$ -glucans). Despite finding no differences in the exposed Glc among all strains (Fig. 4F), the  $\Delta nsdC$  mutant had about a 2- to 3-fold reduction in the exposure of GalNAc,  $\alpha$ -linked mannose, chitin, and  $\beta$ -1,3-glucan compared to the wild-type and complemented strains (Fig. 4G to J). All the three strains have about the same amount of total carbohydrates in their cell wall (Fig. 4K); however, the mutant strain displayed lower exposure of the cell wall sugar components glucosamine, glucose, and NAG (*N*-acetylglucosamine) but increased mannose and galactose relative to the wild-type and complemented strains (Fig. 4L). Interestingly, transmission electron microscopy (TEM) experiments showed that the cell wall of the  $\Delta nsdC$  mutant was about 5-fold thicker than those of the wild-type and complemented strains (Fig. 4M and N; see also Table S3 at <https://doi.org/10.6084/m9.figshare.12931754.v3>). Therefore, NsdC influences fungal cell wall composition organization and structure.

**Chromatin immunoprecipitation of RNA polymerase II coupled to next-generation sequencing (PolII ChIP-Seq) for  $\Delta nsdC$ .** Considering that NsdC has many different functions besides its involvement in the sexual process, we decided to evaluate the transcriptional impact of the lack of *nsdC* after growth in MM for 16 h in the absence and presence of  $CaCl_2$ . To investigate this, we used PolII ChIP-Seq with a corresponding wild-type strain and the  $\Delta nsdC$  mutant. Considering that RNA PolII recruitment is related to transcriptional activity, a corresponding increase and decrease in RNA PolII occupancy indicate upregulation and downregulation of gene expression, respectively (31, 32). In the  $\Delta nsdC$  strain compared with the wild type, we identified an increase in RNA PolII occupancy of 805 genes and reduction of PolII occupancy of 120 genes ( $\log_2FC$  [fold change]  $\geq 1.0$  and  $\leq -1.0$ ; false-discovery rate [FDR] of 0.05; see Table S4 at <https://doi.org/10.6084/m9.figshare.12931754.v3>). FunCat (<https://elbe.hki-jena.de/fungifun/fungifun.php>) enrichment analyses of the upregulated genes demonstrated an increased PolII occupancy for those encoding proteins involved in translation, mitochondrion, aerobic respiration, electron transport, and amino acid metabolism (Fig. 5A). FunCat categorization of the downregulated genes allowed us to identify only a single category of genes, in this case encoding proteins involved in tetracyclic and pentacyclic triterpene (cholesterin, steroid, and hopanoid) metabolism (Fig. 5A).

The same method of transcriptional profiling was then used to compare gene expressions of the  $\Delta nsdC$  and wild-type strains when both were exposed to 200 mM  $CaCl_2$  for 10 min. An increased RNA PolII occupancy was identified for 310 genes together with a reduction of PolII occupancy of 623 genes ( $\log_2FC \geq 1.0$  and  $\leq -1.0$ ; FDR

#### FIG 4 Legend (Continued)

independent biological repetitions. Statistical analysis was performed using a one-way ANOVA compared to the wild-type condition (\*\*,  $P < 0.01$ ; \*\*\*,  $P < 0.001$ ; \*\*\*\*,  $P < 0.0001$ ). (F to J) Detection of sugar exposed on the cell wall. Conidia were cultured in liquid MM until hyphae were produced, UV killed, and stained with WGA (wheat germ agglutinin)-FITC (recognizing surface-exposed glucosamine [Glc]) (F), SBA (soybean agglutinin)-FITC (preferentially binds to oligosaccharide structures with terminal  $\alpha$ - or  $\beta$ -linked *N*-acetylgalactosamine [GalNAc] and, to a lesser extent, galactose residues—important for recognizing galactosaminogalactan [GAG]) (G), ConA (concanavalin A)-FITC (recognizes  $\alpha$ -linked mannose) (H), CFW (recognizing chitin) (I), and soluble dectin-1 staining (recognizing  $\beta$ -glucans) (J). (K) Total carbohydrate concentration in the cell walls of the wild-type,  $\Delta nsdC$ , and  $\Delta nsdC::nsdC^+$  strains. (L) Sugar concentrations in the cell walls as determined by high-performance liquid chromatography (HPLC), in mycelial extracts of the *A. fumigatus* strains when grown for 16 h in MM at 37°C. Experiments were performed in triplicate, and results are displayed as mean values with standard deviations (one-way ANOVA followed by Tukey's *post hoc* test [\*],  $P < 0.05$ ; \*\*,  $P < 0.01$ ; \*\*\*,  $P < 0.001$ ; \*\*\*\*,  $P < 0.0001$ ). (M) Transmission electron microscopy of mycelial sections of *A. fumigatus* wild-type,  $\Delta nsdC$ , and  $\Delta nsdC::nsdC^+$  strains following growth for 24 h in MM at 37°C. Inset shows a magnification of the  $\Delta nsdC$  mutant cell wall. (N) The cell wall thickness (nanometers) of 100 sections of different hyphal germlings (average from 4 sections per germling) was measured. Standard deviations present the average from the 100 measurements, and statistical differences were evaluated by using one-way analysis of variance (ANOVA) and Tukey's *post hoc* test (\*,  $P < 0.05$ ).

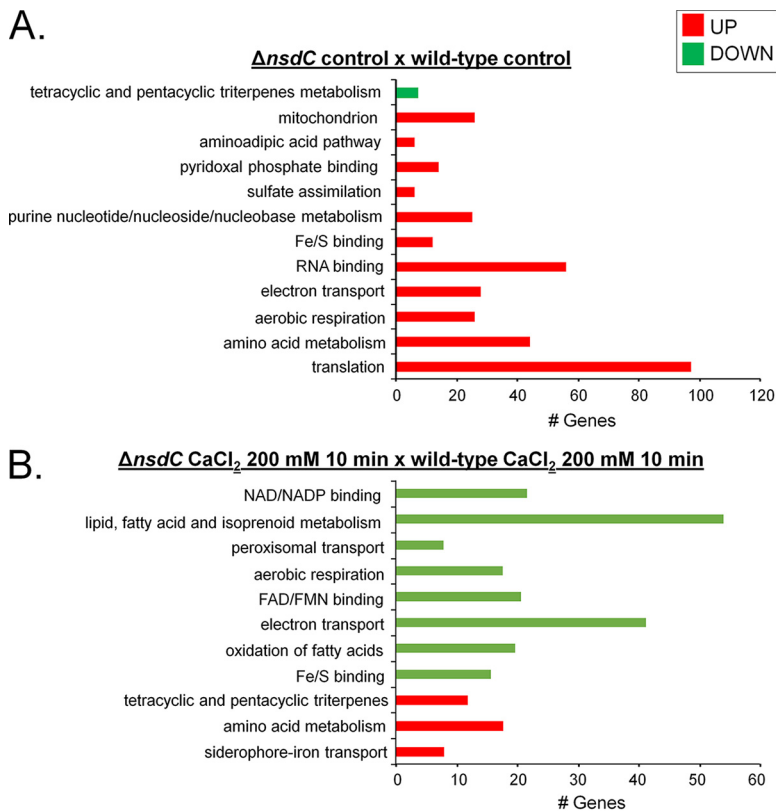


**FIG 5** A summary of the categorization terms of overrepresented up- or downregulated (adjusted  $P$  value  $< 0.05$ ) genes after PolII ChIP-Seq for the  $\Delta nsdC$  strain relative to the parental control. FunCat (<https://elbe.hki-jena.de/fungifun/fungifun.php>) enrichment analyses for the  $\Delta nsdC$  control  $\times$  wild-type control (A) and  $\Delta nsdC$  CaCl<sub>2</sub> (200 mM, 10 min)  $\times$  wild-type CaCl<sub>2</sub> (200 mM, 10 min) (B). FAD/FMN, flavin adenine dinucleotide/flavin mononucleotide.

of 0.05; see Table S4 at <https://doi.org/10.6084/m9.figshare.12931754.v3>). FunCat (<https://elbe.hki-jena.de/fungifun/fungifun.php>) enrichment analyses demonstrated an increased PolII occupancy of genes encoding siderophore-iron transport and amino acid and tetracyclic and pentacyclic triterpene (cholesterin, steroid, and hopanoid) metabolism (Fig. 5B). However, we have not observed any iron deficiency in the  $\Delta nsdC$  strain radial growth (see Fig. S2 at <https://doi.org/10.6084/m9.figshare.12931754.v3>). FunCat categorization of the downregulated genes allowed us to identify proteins involved in Fe/S binding; electron transport; aerobic respiration; lipid, fatty acid, and isoprenoid metabolism; peroxisomal transport; amino acid metabolism; mitochondrial transport; and siderophore-iron transport (Fig. 5B).

We identified at least five genes encoding proteins involved in the sexual process as modulated under both transcriptional conditions (absence or presence of CaCl<sub>2</sub> [Fig. 5A]; also see Table S4 at <https://doi.org/10.6084/m9.figshare.12931754.v3>): (i) *rosA* (AFUA\_4g09710), overexpressed in the presence of CaCl<sub>2</sub>, a repressor of sexual development in *A. nidulans* (33); (ii) *csnC* (AFUA\_2G07340), overexpressed in the absence of CaCl<sub>2</sub>, an *A. nidulans* ortholog that has a role in cleistothecium development and COP9 signalosome localization (34); (iii) *osaA* (AFUA\_3g09640), overexpressed in the presence of CaCl<sub>2</sub>, encoding a protein with a WOPR domain involved in regulation of sexual development in *A. nidulans* (35); (iv) *nsdD* (AFUA\_3g13870), overexpressed both in the absence and in the presence of CaCl<sub>2</sub>, encoding a GATA-type transcriptional activator and required during an early stage of mating (36); and (v) *imeB* (AFUA\_2g13140), overexpressed in the presence of CaCl<sub>2</sub>, a serine/threonine protein kinase involved in the inhibition of sexual development in *A. nidulans* (37).

There are several genes encoding proteins involved in the asexual conidiation

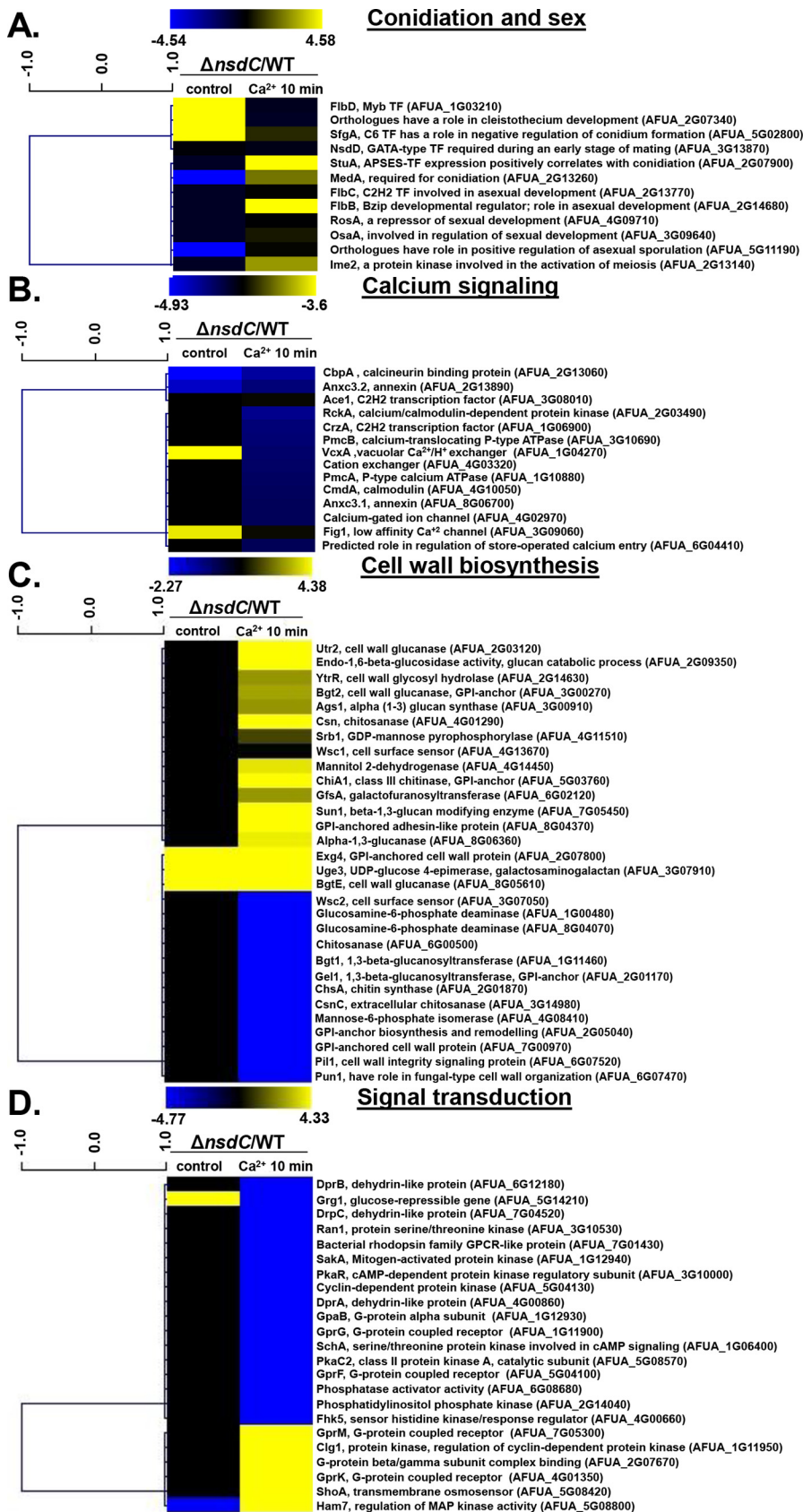
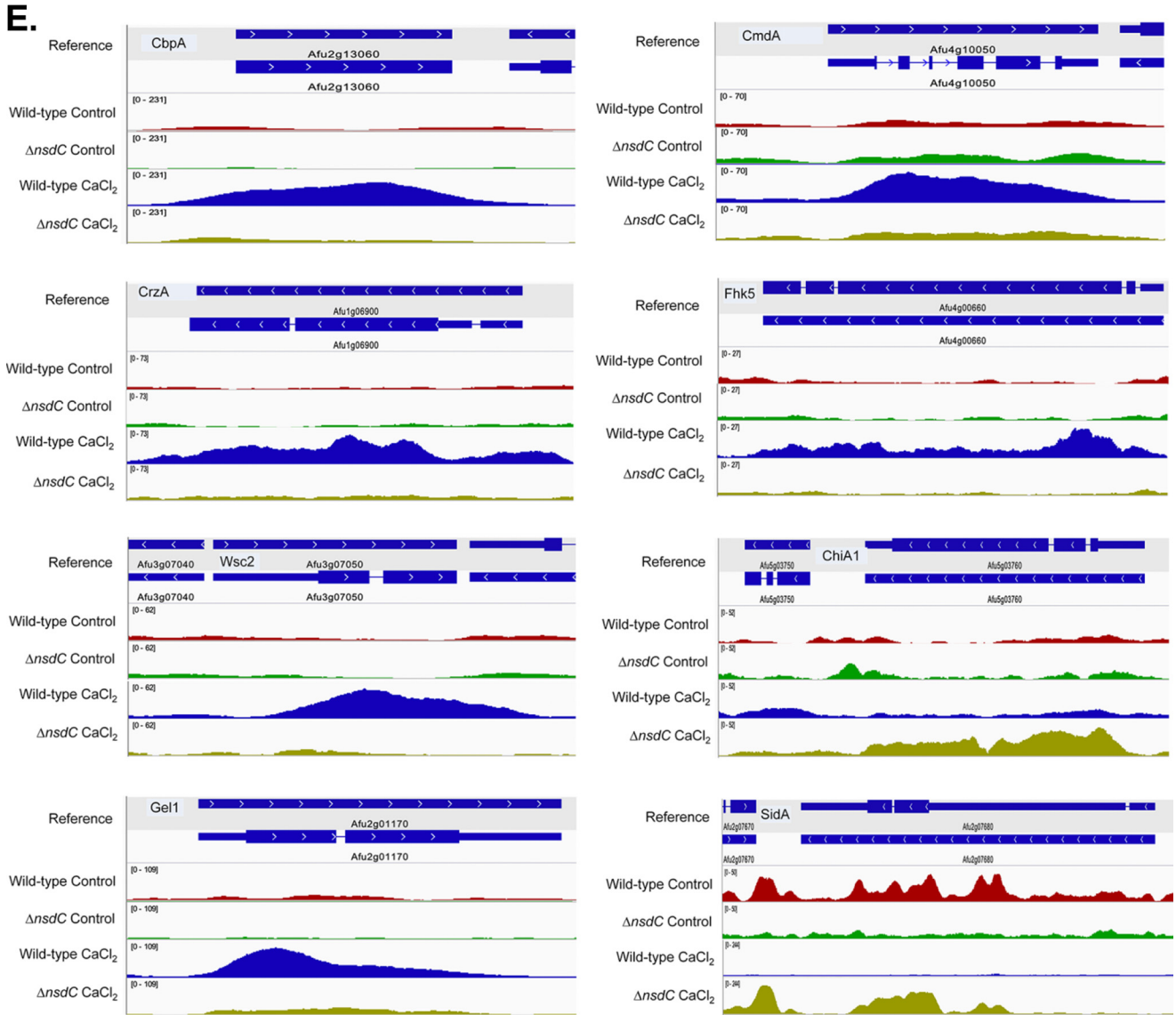
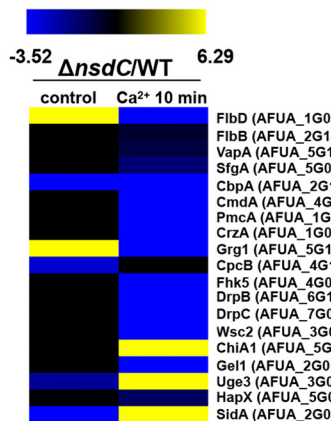
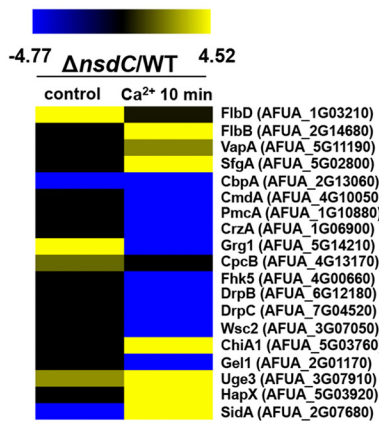


FIG 6 (Continued).



**F. Selected genes PolII ChIP seq**

**G. Selected genes RTqPCR**



**H.**

| RTqPCR x ChIP seq PolII                      |                              |                              |
|--|------------------------------|------------------------------|
|  | $\Delta nsdC$ x WT (control) | $\Delta nsdC$ x WT (calcium) |
| Spearman r                                   | 0.9429                       | 0.6801                       |
| 95% confidence interval                      | -                            | 0.2987 to 0.8742             |
| P value (two-tailed)                         | 0.0167                       | 0.0019                       |
| P value summary                              | *                            | **                           |
| Exact or approximate P value?                | Exact                        | Gaussian Approximation       |
| Is the correlation significant? (alpha=0.05) | Yes                          | Yes                          |

**FIG 6** Independent validation of selected genes identified as modulated in PolII ChIP by RT-qPCR. (A to D) The results show the PolII occupancy for selected annotated genes encoding proteins putatively involved in conidiation and sex (A), calcium signaling (B), cell wall biosynthesis (C), and signal (Continued on next page)

process that are overexpressed in the absence of  $\text{CaCl}_2$  (Fig. 6A; also see Table S4 at <https://doi.org/10.6084/m9.figshare.12931754.v3>), such as *flbD* (AFUA\_1G03210, a Myb family transcription factor whose *A. nidulans* ortholog plays a role in conidiophore development [38]) and *SfgA* (AFUA\_5G02800, a C6 transcription factor that has a role in negative regulation of conidium formation [39]), and in the presence of  $\text{CaCl}_2$ , such as *flbB* (AFUA\_2g16060, a Bzip developmental regulator involved in *A. nidulans* asexual development [40]), *flbC* (AFUA\_2g13770, a  $\text{C}_2\text{H}_2$  finger domain protein involved in asexual development in *A. nidulans* [40]), and *vapA* (AFUA\_5g11190, a component of the plasma membrane-associated VapA-VipC-VapB methyltransferase complex that controls *A. nidulans* differentiation [41]).

Taken together, these results indicate that NsdC is important for amino acid, iron, and lipid metabolism as well as conidiation, impacting several biological responses under basal conditions and upon exposure to calcium stress.

**Independent validation of NsdC influence on transcriptional regulation of calcium response.** RT-qPCR experiments validated the PolII ChIP-Seq results for the majority of the 19 selected genes from conidiation and sex, calcium signaling, cell wall, and signal transduction responses (Fig. 6A to G; see also Table S4 and Fig. S5 at <https://doi.org/10.6084/m9.figshare.12931754.v3>). The *cofA* (Afu5g10570) gene, which encodes the actin-binding protein cofilin, was used as a normalizer due to its consistent expression in all strains during calcium stress (30). The expression of these 19 genes showed a high level of correlation with the PolII ChIP-Seq data (Spearman correlation from 0.6801 to 0.9429 [Fig. 6H]). These results validate that NsdC has functions in modulating the response to calcium stress, affecting directly or indirectly the expression of genes involved in conidiation, sex, signal transduction, and cell wall biosynthesis and/or remodeling.

**The *A. fumigatus*  $\Delta nsdC$  mutant has attenuated virulence in immunodeficient mice.** In the leukopenic BALB/c murine model of invasive pulmonary aspergillosis, wild-type and  $\Delta nsdC::nsdC^+$  exposure resulted in 100 and 80% mortality at 11 and 15 days postinoculation, respectively (Fig. 7A). In contrast, the  $\Delta nsdC$  mutant caused a reduced mortality of only 40% at 15 days postinoculation, which was statistically different from the wild-type and  $\Delta nsdC::nsdC^+$  strains (Mantel-Cox and Gehan-Brestow-Wilcoxon tests;  $P$  values  $< 0.05$  [Fig. 7A]). Additionally, fungal burden in lungs of mice was measured by qPCR and revealed a lower presence of  $\Delta nsdC$  DNA than of that of the wild-type and complemented  $\Delta nsdC::nsdC^+$  strains (Fig. 7B). These data strongly indicated that the lack of NsdC in *A. fumigatus* caused a significant reduction in virulence in immunodeficient mice and also indicated that the  $\Delta nsdC$  strain might be more sensitive to macrophage killing.

Histopathological examination revealed that at 72 h postinfection mouse lungs infiltrated with the  $\Delta nsdC$  strain showed no sign of fungal burden. In contrast, mice infected with the wild-type or the  $\Delta nsdC::nsdC^+$  strain contained multiple foci of invasive hyphal growth, which penetrated the pulmonary epithelium in major airways (Fig. 7E). These data strongly indicated that the lack of NsdC in *A. fumigatus* caused a significant reduction in virulence in immunodeficient mice and also indicated that the  $\Delta nsdC$  strain might be more sensitive to macrophage killing.

Since loss of the *nsdC* gene produced alterations in cell wall composition (Fig. 4), we hypothesized that it could influence the immune host response and virulence.

#### FIG 6 Legend (Continued)

transduction (D). The  $\Delta nsdC$  strain is shown as the deletion strain versus the equivalent wild-type (WT) strain for control and 10-min time point (the mutant values have been normalized to the basal level of expression of each gene before stress, i.e., expression ratios are being compared: the  $\Delta nsdC$  control divided by the wild-type control and the  $\Delta nsdC$  mutant 10 min versus time zero divided by the wild-type 10 min versus time zero). Hierarchical clustering was performed in MeV (<http://mev.tm4.org/>), using Spearman correlation with complete linkage clustering. (E) PolII ChIP-Seq Integrative Genomics Viewer (IGV; <http://software.broadinstitute.org/software/igv/download>) screenshot for selected genes from panels F and G. (F) Heat map for the PolII occupancy of 19 selected genes involved in conidiation and sex, calcium signaling, cell wall biosynthesis, and signal transduction. (G) Heat map of RT-qPCR for the same 19 selected genes from panel F. The wild-type and  $\Delta nsdC$  mutant strains were grown for 20 h at 37°C and transferred to 200 mM  $\text{CaCl}_2$  for 0 and 10 min. Gene expression was normalized using *cofA* (Afu5g10570). Standard deviations present the average of three independent biological repetitions (each with 2 technical repetitions). (H) The expression of these 19 genes as measured by RT-qPCR showed a high level of correlation with the PolII ChIP-Seq data (Spearman correlation from 0.6801 to 0.9429).

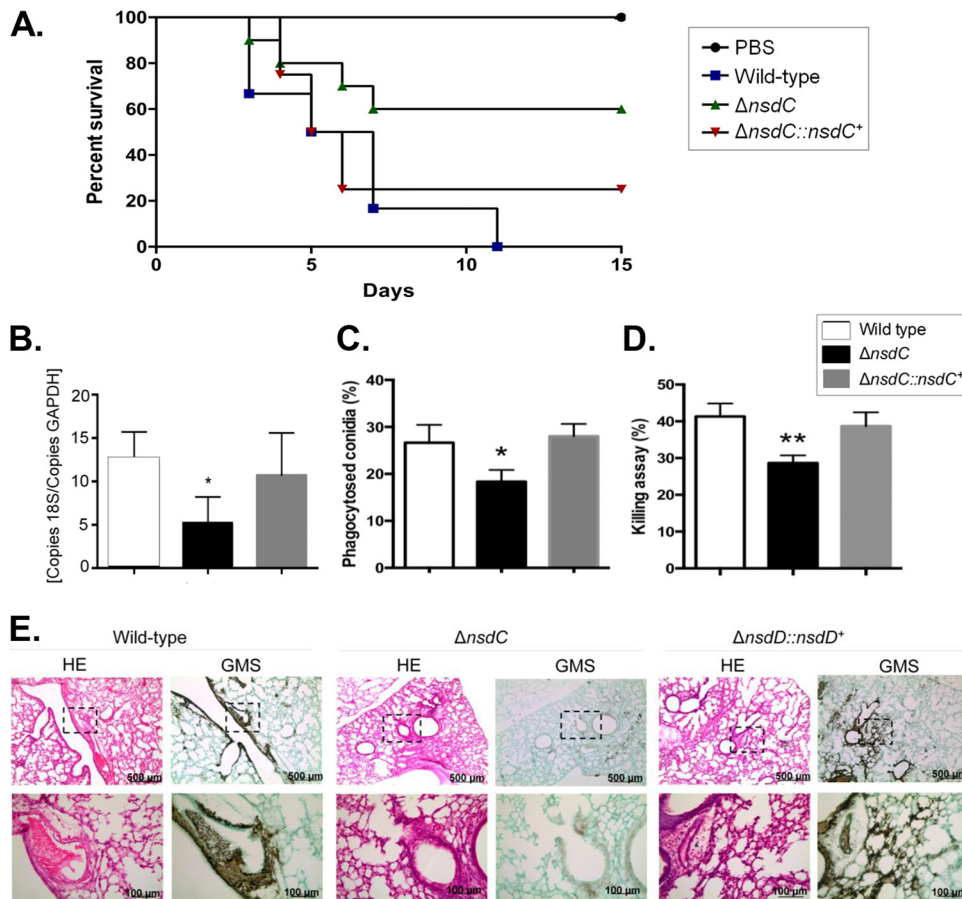


**FIG 7** The *A. fumigatus*  $\Delta nsdC$  strain has attenuated virulence in neutropenic mice. (A) Comparative analysis of wild-type,  $\Delta nsdC$ , and  $\Delta nsdC::nsdC^+$  strains in a neutropenic murine model of pulmonary aspergillosis. Mice in groups of 10 per strain were inoculated intranasally with a 20- $\mu\text{l}$  suspension of conidia at a dose of  $10^5$ . PBS, phosphate-buffered saline. The statistical significance of comparative survival values was calculated with the Prism statistical analysis package by using log rank (Mantel-Cox) and Gehan-Brestow-Wilcoxon tests. (B) Fungal burden was determined 48 h postinfection by real-time qPCR based on the 18S rRNA gene of *A. fumigatus* and an intronic region of the mouse GAPDH gene. Fungal and mouse DNA quantities were obtained from the  $C_T$  values from an appropriate standard curve. Fungal burden was determined through the ratio between nanograms of fungal DNA and milligrams of mouse DNA. The results are the means ( $\pm$  standard deviations) from five lungs for each treatment. Statistical analysis was performed by using the *t* test (\*,  $P < 0.05$ ). (C and D) Fungal killing capacity of mouse bone marrow-derived macrophages (BMDMs) assessed as CFU of surviving *A. fumigatus* strains (wild type,  $\Delta nsdC$ , or  $\Delta nsdC::nsdC^+$  mutant) after 4 h of infection. The percent killing was calculated from CFU remaining compared with control samples without macrophages. The results are the means ( $\pm$  standard deviation) of three independent biological repetitions. Statistical analysis was performed using a one-way ANOVA compared to the wild-type condition (\*,  $P < 0.05$ ; \*\*,  $P < 0.01$ ). (E) Histopathology of mice infected with *A. fumigatus* wild-type or  $\Delta nsdC$  or  $\Delta nsdC::nsdC^+$  mutant strain. GMS (Grocott's methenamine silver) and HE (hematoxylin and eosin) staining of lung sections representative of infections. The boxed area from the top row is magnified in the bottom row. Bars, 100 and 500  $\mu\text{m}$ .

Macrophages contribute to innate immunity, fungal clearance, and the generation of a proinflammatory response during *A. fumigatus* exposure to the microbe (42). Thus, the capacity of bone marrow-derived macrophages (BMDMs) to phagocytose and kill the wild-type,  $\Delta nsdC$ , and  $\Delta nsdC::nsdC^+$  conidia was assessed. The *nsdC* mutant conidia presented lower killing rates by BMDMs than did the wild-type and *nsdC::nsdC^+* conidia (Fig. 7C and D). These results indicate that the *nsdC* mutant was less susceptible to macrophage killing.

In addition, experiments with immunocompetent C57BL/6 mice were performed to assess the ability of the  $\Delta nsdC$  strain to generate an inflammatory response. The immunocompetent mice were inoculated with  $5 \times 10^7$  conidia of wild-type,  $\Delta nsdC$ , and  $\Delta nsdC::nsdC^+$  strains by the intratracheal (i.t.) route. After 72 h of inoculation, the lung-

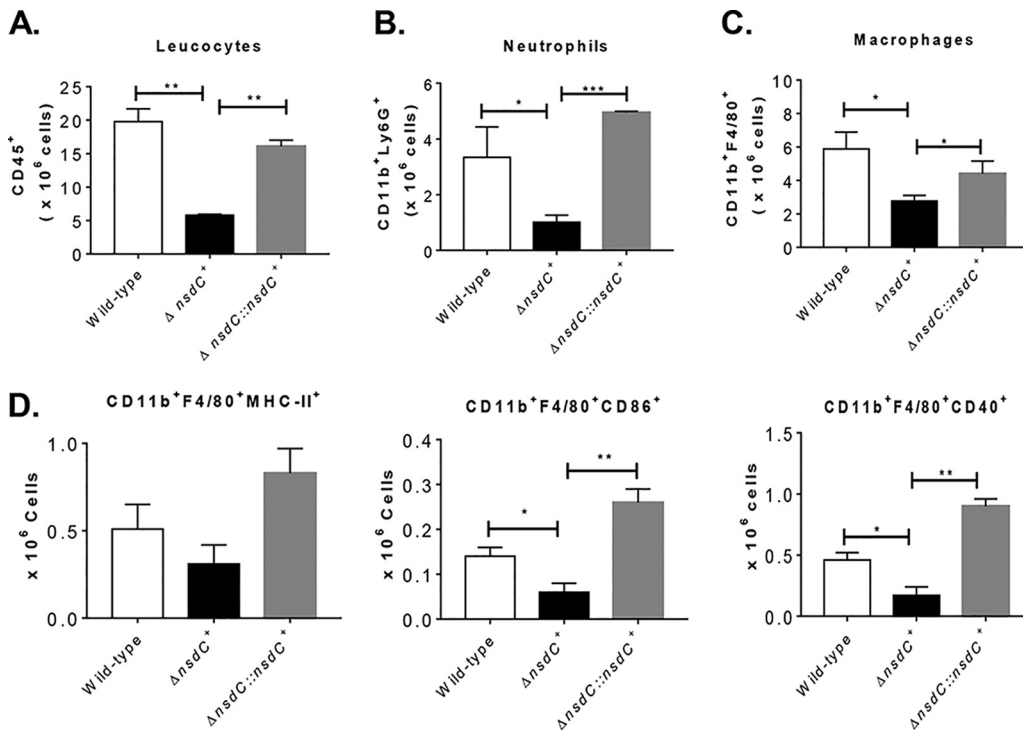


**FIG 8** *ΔnsdC* determines impaired leukocyte influx to the lungs of immunocompetent C57BL/6 mice. Mice were inoculated with  $5 \times 10^7$  conidia of *A. fumigatus* strains by i.t. route, and cell phenotypes were determined after 72 h of infection. Lungs from mouse groups ( $n=3$ ) were excised and digested enzymatically. Cell suspensions were obtained and stained as described in Materials and Methods. The stained cells were analyzed immediately on a FACSLyric flow cytometer with gating of granulocytes, as judged from forward scatter (FSC) and side scatter (SSC). The number of total CD45<sup>+</sup> leukocytes (A), CD11b<sup>+</sup> F4/80<sup>+</sup> Ly6G<sup>+</sup> neutrophils (B), CD11b<sup>+</sup> F4/80<sup>+</sup> macrophages (C), and inflammatory macrophages (CD11b<sup>+</sup> F4/80<sup>+</sup> MHC-II<sup>+</sup>, CD11b<sup>+</sup> F4/80<sup>+</sup> CD86<sup>+</sup>, and CD11b<sup>+</sup> F4/80<sup>+</sup> CD40<sup>+</sup>, respectively) (D) was assessed. One hundred thousand cells were counted, and the data are expressed as number of positive cells. Data are expressed as means  $\pm$  standard errors (SE) of the mean and are representative of two independent experiments (\*,  $P < 0.05$ , and \*\*,  $P < 0.01$ ).

infiltrating leukocytes were obtained and analyzed for the expression of surface molecules of leukocytes by flow cytometry. As shown in Fig. 8A to D and also in Fig. S3 at <https://doi.org/10.6084/m9.figshare.12931754.v3>, lower numbers of total leukocytes (CD45<sup>+</sup> cells), neutrophils, and macrophages were found in the lungs of mice exposed to *ΔnsdC* mutant strains compared with wild-type and *ΔnsdC::nsdC*<sup>+</sup> conidium inoculation. Similarly, fewer numbers of inflammatory macrophage cells (CD11b<sup>+</sup> F4/80<sup>+</sup> major histocompatibility complex class II [MHC-II<sup>+</sup>], CD11b<sup>+</sup> F4/80<sup>+</sup> CD86<sup>+</sup>, and CD11b<sup>+</sup> F4/80<sup>+</sup> CD40<sup>+</sup>, respectively) were detected in the lungs of mice inoculated with *ΔnsdC* mutant strains compared with wild-type and *ΔnsdC::nsdC* controls. These data strongly indicate that the lack of NsdC in *A. fumigatus* caused a significant reduction in virulence in immunodeficient and immunocompetent mice and also indicated that the *ΔnsdC* strain was more sensitive to macrophage killing.

## DISCUSSION

A family of 20 Nsd mutants were first identified in *A. nidulans* and named based on the fact that they failed to produce cleistothecia, i.e., were never in sexual development (43, 44). Of these mutants, only the NsdC and NsdD mutants have so far been characterized (29, 44, 45). Partly due to the nomenclature used, both the *nsdC* and *nsdD* genes are known primarily for their essential role in sexual reproduction (27). However, results from the present study, combined with reevaluation of previous studies of *nsdC* gene function, reveal that the NsdC transcription factor in particular has

much more broad biological functions beyond simply promotion of sexual reproduction, as will now be described.

An indication of one of the additional functions of NsdC came recently from a study aiming to identify new transcription factors involved in the calcium stress response in *A. fumigatus* (30). Large-scale phenotypic screenings have been widely used to identify new components of signaling pathways and to study drug resistance mechanisms (46–49). A library of null-mutant transcription factors was challenged with high concentrations of  $\text{CaCl}_2$ , and this resulted in the identification of an *A. fumigatus*  $\Delta\text{nsdC}$  mutant with increased sensitivity to  $\text{CaCl}_2$  relative to the wild-type parental strain, suggesting a role for NsdC in calcium response. Additional work in the present study demonstrated that complementation with a functional *nsdC* gene restored the wild-type phenotype. Further phenotyping assays then showed that loss of *nsdC* led to cyclosporine (a calcineurin-inhibitory drug) resistance. These combined results indicate a first additional important role for NsdC in mediating calcium tolerance. Whether this involves a direct or indirect link to the central calcium-calcineurin-CrzA pathway requires further investigation. Additional experiments are necessary to characterize the interactions among these different TFs and calcineurin. Interestingly, transcriptional profiling using PolII ChIP-Seq showed at least 933 changes in gene expression between the  $\Delta\text{nsdC}$  mutant and the wild type when exposed to calcium stress, indicating a possible wide spectrum of activity for NsdC in calcium response. However, most of these changes are in increased gene expression (805 changes), suggesting that NsdC could act as a repressor.

Given that *nsdC* was first identified in *A. nidulans* due to a total lack of sexual development (including failure to produce Hülle cells as well as cleistothecia) even under conditions which favor fruiting body formation by single isolates (29), we then wished to determine whether NsdC had a similar role in sexual development of *A. fumigatus*. Despite sexual development being demonstrated in *A. fumigatus* under laboratory conditions (22), most advances in understanding the regulation of the sexual cycle in *Aspergillus* species have come from studies using the model *A. nidulans* (27, 44, 50). However, notable differences in the breeding systems of the species (*A. fumigatus* is heterothallic whereas *A. nidulans* is homothallic) suggested that findings from *A. nidulans* might not necessarily be applicable to *A. fumigatus*. Therefore, both *MAT1-1* and *MAT1-2*  $\Delta\text{nsdC}$  mutant strains of *A. fumigatus* were constructed in a high-fertility genetic background to assess the contribution of NsdC in sexual reproduction in this species. It was found that, provided one of the *MAT1-1* or *MAT1-2* mating partners contained a functional copy of *nsdC*, the sexual cycle could be completed, leading to cleistothecium and ascospore production, i.e., the absence of NsdC in one mating partner could be complemented by the presence of NsdC produced by the other partner. Indeed, in the original work of Kim et al. (29) it was found that despite the failure to undergo sexual development under selfing conditions, an *nsdC* deletion mutant of *A. nidulans* was nevertheless still able to outcross to a compatible auxotrophic strain of *A. nidulans* with a functional copy of *nsdC*, mirroring our findings with *A. fumigatus*. The exact mechanism of complementation is unclear, but it can be speculated that the partner with the functional copy of *nsdC* might act as the maternal partner, forming ascogonial coils (and later maternal tissues) that could be fertilized by the male  $\Delta\text{nsdC}$  partner, given that *nsdC* is thought to act at a very early stage of sexual development (27, 29). Alternatively, the partner with the functional copy of *nsdC* might allow hyphal fusions necessary for sex to occur, with this ability missing from  $\Delta\text{nsdC}$  strains. It has proved difficult to determine the early morphological stages of sexual development in *A. fumigatus* (K. M. Lord, N. D. Read, and P. S. Dyer, unpublished results), although putative ascogonial coils have been described in *A. nidulans* (51). However, if both the *MAT1-1* and *MAT1-2* mating partners of *A. fumigatus* were of the  $\Delta\text{nsdC}$  genotype, then sexual fertility was totally abolished. This was a significant result, as it demonstrated that NsdC has a second, essential positive regulatory role for sexual development in *A. fumigatus*, as observed for its counterpart in *A. nidulans* (29). NsdC has also been shown to have a role in sexual development in *A. flavus*, where its deletion led to

inhibition of formation of sclerotia, these structures being an important first stage in the sexual cycle (27, 52).

These findings also provide a key precedent when evaluating the function of genes in sexual development in the heterothallic *A. fumigatus*, in that it will be important to disrupt the gene(s) under study in both mating partners to conclusively evaluate gene function. Indeed, it is noted that the function of genes in sexual development is generally performed with homothallic species such as *A. nidulans*, *Sordaria macrospora*, and *Fusarium graminearum* (27, 53, 54) as this removes the time-consuming need to delete a gene(s) in both partners, which is the case for heterothallic species. However, there may be exceptions such as studies of functionality of mating-type genes, as distinct *MAT1-1* and *MAT1-2* idiomorph genes are found in the different mating partners (20, 25, 55). Also, in contrast to the current results for *nsdC*, the loss of the *nsdD* gene (another transcription factor involved in sexual reproduction in the aspergilli) in one mating partner alone was enough to suppress fruit body formation in *A. fumigatus* (25).

In the original study of *nsdC* function in *A. nidulans*,  $\Delta nsdC$  mutants were also found to be characterized by retarded vegetative growth compared to the wild type, with an approximately 30% reduction in growth rate (29). A very similar result was found in the present study, with the *A. fumigatus*  $\Delta nsdC$  strains in both the CEA17 and supermater genetic backgrounds showing a reduction in vegetative growth rate on solid media. However, this growth difference is observed only in minimal medium and not in complete medium, suggesting the  $\Delta nsdC$  mutant has metabolic deficiencies that are supplemented by the complete medium chemical composition. Taken together, these results confirm a third important role for NsdC in the promotion of vegetative growth. This conclusion is supported in part by the gene expression studies from the present study, involving PolII ChIP-Seq, which showed that NsdC is associated with the regulation of several biological processes under basal growth conditions. It is speculated that the upregulation of some biological functions in the  $\Delta nsdC$  mutant was perhaps to counterbalance the loss of NsdC. Interestingly, biosynthesis of different aspects of secondary metabolism was up- and downregulated in the  $\Delta nsdC$  mutant, implying a regulatory function of NsdC in secondary metabolite production as has been observed in *Aspergillus flavus* (52).

In the original study of *nsdC* function in *A. nidulans*,  $\Delta nsdC$  mutants were furthermore found to be characterized by “hyperactive” asexual sporulation, with earlier-than-normal development of conidia, and conidiation even in liquid media, indicating that NsdC negatively regulates asexual reproduction (29). A very similar result was found in the present study with *A. fumigatus*, with microscopic examination revealing the production of conidiophores and conidia in the  $\Delta nsdC$  mutant when grown in liquid MM, conditions under which the parental wild type failed to produce conidia. This activity of NsdC appears to be explained in part as a result of repression of *brlA* expression. *BrlA* is a key regulator of asexual sporulation due to its activity in controlling the initiation of conidiophore development (6, 9, 11, 56). It was found that *brlA* mRNA accumulated in the  $\Delta nsdC$  strain after 24 h of growth in liquid MM, unlike the parental strain. Higher *brlA* expression has also been observed in an  $\Delta nsdC$  mutant of *A. flavus* (which also exhibited altered conidiophore morphology), and *brlA* transcripts were found to be expressed earlier (but in similar quantities) in an *A. nidulans*  $\Delta nsdC$  mutant (29, 52). Transcriptional profiling also indicated that several genes important for conidiation, such as *flbB*, *flbC*, and *flbD*, have increased expression in the  $\Delta nsdC$  mutant. Meanwhile, our group and others have previously described a role of the MAP kinase *MpkB* in the negative regulation of asexual development in both *A. fumigatus* and *A. nidulans*, whereby  $\Delta mpkB$  mutants produced conidia in submerged cultures with a constant accumulation of *brlA* mRNA (18, 57). In the present study, we observed an accumulation of *nsdC* mRNA in the  $\Delta mpkB$  strain of *A. fumigatus*, indicating negative control of *nsdC* expression by *MpkB*. Further investigation is required in order to establish if *MpkB* also influences sexual development in *A. fumigatus*, as already described for *A.*

*nidulans* (28). Taken together, these results confirm a fourth important role for NsdC in the negative regulation of asexual reproduction by transcriptional repression of *brlA*, subject to control by MpkB.

Cell wall composition and structure vary substantially with cell cycle progression and in response to environmental changes (58). Very little is known about *A. fumigatus* TFs regulating cell wall biosynthesis and/or remodeling. *A. fumigatus* TFs such as RlmA and calcium-calcieneurin-dependent TFs such as CrzA and ZipD have been characterized in more detail as regulating several genes involved in the cell wall metabolism (30, 49, 59–66). In the present study, deletion of the *nsdC* gene led to greater sensitivity to cell wall-damaging agents, a reorganization of cell wall structure, decreased and increased cell wall sugar content, and increased cell wall width. The *A. fumigatus* cell wall is composed of more than 90% polysaccharides, with the core skeleton composed by a branched  $\beta$ -1,3-glucan linked to chitin, galactomannan, and  $\beta$ -1,3- $\beta$ -1,4-glucans;  $\alpha$ -1,3-glucan and mannans act as a cement, filling the pores between fibrillar polysaccharides (67). We have observed no differences in total carbohydrates isolated from the cell walls of the wild-type,  $\Delta nsdC$ , and complemented strains. However, there are increased concentrations of mannose and galactose and decreased concentrations of glucosamine, glucose, and NAG present in the  $\Delta nsdC$  cell walls compared to the wild-type and complemented strains. It proved difficult to establish a direct relationship between the organization and composition of the fungal cell wall that could directly explain the observed increased thickness of  $\Delta nsdC$  cell walls. It is possible that the combination of the increased and decreased sugar concentrations could impact the  $\Delta nsdC$  cell wall organization, increasing the cell wall width. Transcriptional profiling also showed that several genes involved in the cell wall biosynthesis and remodeling were dysregulated in the  $\Delta nsdC$  mutant. Cell wall thickening has also been linked to defects in sphingolipid metabolism in *A. nidulans* and yeasts (68), but alteration of cell membrane components was not assessed in this work. Interestingly, transcriptional profiling found up- and downregulated genes involved in lipid, fatty acid, and isoprenoid metabolism, which could help to explain this striking phenotype. In contrast, loss of *nsdD* in *A. fumigatus* conferred resistance toward certain cell wall stressors (25). Taken as a whole, these results demonstrate a fifth important role for NsdC in response to cell wall stress and correct cell wall organization. More studies are necessary to understand how NsdC interacts with RlmA, CrzA, and ZipD; is regulated by calcineurin; and populates the promoter regions of the genes encoding proteins important for the cell wall integrity pathway.

Cell wall organization impacts directly virulence and host immune recognition in *A. fumigatus* (69). Accordingly, leukopenic mice inoculated with  $\Delta nsdC$  conidia showed a reduction in mortality, fungal burden, and inflammation compared to inoculation with the wild-type parental strain, possibly also linked to the lower growth rate of the  $\Delta nsdC$  strain. Despite the reduced virulence,  $\Delta nsdC$  conidia were less well recognized by macrophages than wild-type conidia, probably because of the increased thickness of the cell wall in this mutant which possibly masks  $\beta$ -1,3-glucan (which is already reduced in the mutant) and other cell wall components responsible for triggering immune response in the host (70). As a result,  $\Delta nsdC$  conidia were also less efficiently eliminated. This impaired interaction between macrophages and  $\Delta nsdC$  conidia likely resulted in fewer inflammatory cytokines and consequently a diminished influx of leukocytes to the site of inoculation as further confirmed by results from the immunocompetent model of pulmonary acute aspergillosis included in the present study. Corroborating the lower phagocytosis index, the killing rates may be influenced not just because the conidia were not killed but also because the conidium ingestion was affected. However, a compromised phagocytosis associated with an efficient macrophage activity would affect the recruitment of immune cells as shown in Fig. 6A. The impaired interaction between alveolar macrophages and the *nsdC* mutant strain likely resulted in reduced inflammatory signals and consequently less influx of leukocytes to the site of infection as we showed in Fig. 6. In addition, the

diminished expression of activation markers (Fig. 6D) clearly showed that mechanisms of macrophage activation were impaired against the *nsdC* mutant strain. We believe that the cell wall organization impacts directly virulence and host immune recognition by innate immune cells during *A. fumigatus* infection. These findings were previously described and revised by reference 69. These results demonstrate an extra sixth role for NsdC in virulence and host immune recognition.

In summary, in addition to its known essential roles in sexual reproduction and control of growth rate and asexual reproduction, we have shown in the present study of *A. fumigatus* that the NsdC transcription factor has additional previously unrecognized biological functions including calcium tolerance, cell wall stress response, and correct cell wall organization and functions in virulence and host immune recognition. Indeed, the fact that NsdC is needed for correct vegetative growth and that gene deletion resulted in changes in expression of over 620 genes under basal growth conditions suggests that promotion of sexual reproduction is perhaps not the principal role of NsdC (despite the gene epithet) and that instead this transcription factor mediates the activity of a wide variety of key signaling and metabolic pathways. In contrast, deletion of many other genes in *A. nidulans* with a principal role in sexual reproduction has little impact on vegetative growth (27). In addition, whereas overexpression of the key sex-related genes *veA* and *nsdD* resulted in induction of sex in submerged cultures of *A. nidulans*, no such effect was seen with overexpression of *nsdC*, again consistent with a primary role other than sexual reproduction (29). The multifunctionality of NsdC has been proposed to be linked to the transcription of two different mRNA forms from the *nsdC* gene in *A. nidulans*, with a 3.0-kb form staying relatively constant during the life cycle whereas a shorter, 2.6-kb form accumulated differentially especially during sterigma and sexual development (29). Further research is now warranted into how gene expression is controlled by the NsdC transcription factor.

## MATERIALS AND METHODS

**Strains and media.** All strains used in this study are listed in either Table S1 or Table S5 at <https://doi.org/10.6084/m9.figshare.12931754.v3>. Strains for genetic manipulation were grown at 37°C in either complete medium (YG: 2% [wt/vol] glucose, 0.5% [wt/vol] yeast extract, trace elements) or minimal medium (MM: 1% [wt/vol] glucose, original high-nitrate salts, trace elements, pH 6.5). Solid YG and MM were the same as described above except that 2% (wt/vol) agar was added. Trace elements, vitamins, and nitrate salts compositions were as described previously (71). When required, MM was supplemented at stated concentrations with calcium chloride (CaCl<sub>2</sub>), cyclosporine, sorbitol, nikkomycin Z, Congo red (CR), calcofluor white (CFW), and caspofungin. Strains for sexual reproductive purposes were grown at 28°C on *Aspergillus* complete medium for production of conidia for mating inoculum (20). For characterization of phenotype, plates were inoculated with 10<sup>4</sup> spores per strain and left to grow for 120 h at 37°C.

**Construction of *A. fumigatus* mutants for  $\Delta nsdC$  growth assays and NsdC-GFP localization.** To generate the NsdC-GFP::pyrG fusion fragment, a 3-kb portion of DNA consisting of the *nsdC* open reading frame (ORF) and 5' untranslated region (UTR), along with a 1-kb segment of DNA consisting of the 3' UTR flanking region, was amplified with primers *nsdC* pRS426 5fw/*nsdC* orf LINKER GFP rv and *nsdC* 3utr pyrG 3fw/*nsdC* pRS426 3rv, respectively, from CEA17 genomic DNA (gDNA). The 3.3-kb linker-GFP-trpC-pyrG fusion was amplified with primers OZG916 and OZG964 from the pOB435 plasmid. The cassette was generated by transforming each fragment along with the plasmid pRS426 cut with BamHI/EcoRI into the *Saccharomyces cerevisiae* strain. This cassette was then transformed into the CEA17 strain, and verification of NsdC tagging was confirmed via PCR. Figures S4 and S5 at <https://doi.org/10.6084/m9.figshare.12931754.v3> show the confirmatory PCR and Southern blots for the deletion, complementation, and GFP fusion strains. All primers used above are described in Table S6 at <https://doi.org/10.6084/m9.figshare.12931754.v3>.

**Microscopy.** Conidia from the NsdC-GFP strain were cultivated on coverslips in 4 ml of MM for 16 h at 30°C before treatment with 200 mM CaCl<sub>2</sub> for 15 min, 0.25  $\mu$ g/ml cyclosporine for 30 min, or 0.25  $\mu$ g/ml cyclosporine for 30 min and 200 mM CaCl<sub>2</sub> for 15 min. For colocalization experiments, germlings were costained with Hoechst stain (12  $\mu$ g/ml) (Life Technologies, Inc.) for 3 min. Coverslips were inspected on an Observer Z1 fluorescence microscope (Carl Zeiss) using the 100 $\times$  objective oil immersion lens (for GFP, filter set 38 HE, excitation wavelength of 450 nm to 490 nm, and emission wavelength of 525 nm to 550 nm; for Hoechst stain, filter set 49 HE, excitation wavelength of 365 nm, and emission wavelength of 420 nm to 470 nm). Differential interference contrast (DIC) images and fluorescent images were captured with an AxioCam camera (Carl Zeiss, Inc.) and processed using the AxioVision software (version 4.8).

**Conidium count.** Freshly harvested conidia (1  $\times$  10<sup>4</sup>) of the wild-type and  $\Delta nsdC$  and  $\Delta nsdC::nsdC^+$  mutant strains were inoculated onto solid MM at 37°C for 5 days. After this period of growth, four circular sections of the same size were taken from each plate (approximately 1 cm in diameter each) and

placed in a Falcon tube containing 10 ml of a 0.01% Tween solution. Conidia were counted after intensive vortexing using a Neubauer chamber. The assay was performed in triplicate.

**Generation of  $\Delta nsdC$  mutants in a high-fertility *MAT1-1* background.** The highly fertile *A. fumigatus* *MAT1-1* strain 47-51 (synonym AfIR974 [22]) was used as a recipient strain to generate an  $\Delta nsdC$  mutant. The *nsdC* deletion construct was amplified by Phusion polymerase (Thermo) from plasmid pRS426 with primers Af\_*nsdC*Sma\_up\_f and Af\_*nsdC*Sma\_do\_r (see Table S6 at <https://doi.org/10.6084/m9.figshare.12931754.v3>), resulting in a PCR product with flanking *Sma*I restriction sites. The fragment was cloned into the pJET1.2 PCR cloning vector (Thermo) and amplified in *Escherichia coli* DH5 $\alpha$  cells. Plasmid DNA was isolated by using the NucleoSpin plasmid isolation kit (Macherey-Nagel) and restricted with *Sma*I (FastDigest; Thermo) to release the *nsdC* deletion cassette from the plasmid backbone. The 4,345-bp deletion construct, including the pyrithiamine resistance cassette *ptrA* flanked by the upstream and downstream noncoding regions of the *nsdC* gene, was purified from a 1% agarose gel using the GeneJET gel extraction kit (Thermo), and about 2.5  $\mu$ g of DNA was used for a polyethylene glycol (PEG)-mediated transformation of *A. fumigatus* strain 47-51 as described previously (72), with the exception that a mixture of 1.2 g VinoTaste Pro (Novozymes), 0.1 g lysing enzymes from *Trichoderma harzianum* (Sigma), and 0.1 g Yatalase (TaKaRa/Clontech) was used for the generation of protoplasts. Transformants were selected by the presence of 0.1  $\mu$ g/ml pyrithiamine (Sigma) in the regeneration medium. Transformants were subsequently analyzed for gene deletion by Southern blot analysis. A digoxigenin (DIG)-labeled probe against the *nsdC* upstream region was amplified by *Taq* polymerase (New England Biolabs) with primers Af\_*nsdC*Sma\_up\_f and *nsdC*Af\_up\_r (see Table S6 at <https://doi.org/10.6084/m9.figshare.12931754.v3>) and a nucleotide mix containing DIG-11-dUTP. Genomic DNA of wild type and transformants was restricted with *Eco*RI, separated on a 0.8% agarose gel, blotted on a nylon membrane, and hybridized with the digoxigenin-labeled probe. Bands were visualized by using antidigoxigenin Fab fragments linked to alkaline phosphatase and developed by using the chemiluminescent substrate CDP-Star (Sigma). Transformants showing a single band and a shift of the wild-type signal from 5.3 kb down to 2 kb were used in subsequent experiments.

**Generation of  $\Delta nsdC$  mutants with a *MAT1-2* background.** To test the fertility of the  $\Delta nsdC$  mutants in the *MAT1-1* background of the high-fertility strain 47-51 and to generate *nsdC* mutants with a *MAT1-2* background, sexual crosses were set up with high- to medium-fertility *MAT1-2* strains of *A. fumigatus*, namely, strains 47-55 (synonym AfIR964 [22]) and 47-107 (S. S. Swilaiman, G. Szakacs, and P. S. Dyer, unpublished data) (see Tables S1 and S2 at <https://doi.org/10.6084/m9.figshare.12931754.v3>). Crosses were set up on oatmeal agar at 30°C as described by Ashton and Dyer (24) with four replicate 9-cm petri plates per cross, together with control crosses with the 47-51 parent. After 3 to 4 months of incubation, total numbers of cleistothecia per plate were counted using a dissecting microscope and "hoovering" conidia from plates to ensure that any cleistothecia were visible (23, 24). Cleistothecia were collected, and ascospores were released into 100  $\mu$ l sterile 0.05% Tween 80. Ascospores were then heated for 1 h at 70°C to inactivate remaining conidia and vegetative hyphae and to simultaneously induce germination of ascospores (22, 24). Ascospores were plated on *Aspergillus* minimal medium with 50 mM glucose as a carbon source and 10 mM glutamine as a nitrogen source (73) in the presence or absence of 0.1  $\mu$ g/ml of pyrithiamine, given that pyrithiamine resistance was indicative of deletion of the *nsdC* gene. The mating type of individual colonies was subsequently determined by multiplex PCR as previously described (20).

**Fertility analyses of  $\Delta nsdC$  mutants with either *MAT1-1* or *MAT1-2* mating-type background.** Sexual offspring of *MAT1-1* or *MAT1-2* mating type which were of the  $\Delta nsdC$  genotype were analyzed for sexual fertility in crossing experiments with either wild type or  $\Delta nsdC$  mutants of the opposite mating type. This included the use of an additional high-fertility *MAT1-1* isolate, 47-267 (see Table S1 at <https://doi.org/10.6084/m9.figshare.12931754.v3>), for testing of the fertility of *MAT1-2* isolates. Four replicate 9-cm petri plates were set up for each cross. The level of fertility was evaluated by counting total numbers of cleistothecia per crossing plate as described above. Resultant data were analyzed using Prism 8.0 by one-way analysis of variance (ANOVA) and nested one-way ANOVA as appropriate.

**RNA extraction and gene expression analysis.** Strains were grown from  $1 \times 10^7$  conidia in MM for 24 h (wild-type,  $\Delta nsdC$ ,  $\Delta nsdC::nsdC^+$ , and  $\Delta mpkB$  strains) or 48 h (wild-type and  $\Delta mpkB$  strains) at 37°C. Mycelia were ground to a fine powder in liquid N<sub>2</sub>, and total RNA was extracted with TRIzol reagent (Thermo Scientific) according to the manufacturer's protocol. DNA was digested with Turbo DNase I (Ambion Thermo Scientific) according to the manufacturer's instructions. Two micrograms of total RNA per sample was reverse transcribed with the High-Capacity cDNA reverse transcription kit (Thermo Scientific) using oligo dTV and random primer blend, according to manufacturer's instructions. qRT-PCRs were run in a StepOne Plus real-time PCR system (Thermo Scientific) using a Power Sybr green PCR master mix (Thermo Scientific). Three independent biological replicates were used, and the mRNA quantity relative fold change was calculated using standard curves (74). All values were normalized to the expression of the *A. fumigatus tubA* gene. Primers are described in Table S6 at <https://doi.org/10.6084/m9.figshare.12931754.v3>.

**PoII chromatin immunoprecipitation coupled to DNA sequencing (PoII ChIP-Seq).** Conidia ( $1 \times 10^7$ ) of the CEA17 and  $\Delta nsdC$  strains were grown in liquid MM for 16 h at 37°C under shaking conditions. Mycelia and chromatin were prepared as previously described (75). Briefly, formaldehyde was added to the culture to a final concentration of 1% and incubated with gentle rocking for 20 min at room temperature for DNA cross-linking. After, glycine was added to a final concentration of 1 M and the culture was incubated for another 10 min to stop the reaction. Cells were filtered using Miracloth, washed twice with 100 ml of cold water, and rapidly frozen in liquid nitrogen. Thirty milligrams of the frozen mycelia were freeze-dried for at least 2 h and lysed in 800  $\mu$ l of FA lysis buffer for 3 min using a

Bullet blender (Next Advance). Lysis was repeated six times with a 3-min incubation on ice in between. The lysed mycelium was pelleted by centrifugation at 14,000 rpm for 15 min at 4°C and subsequently resuspended in 500  $\mu$ l of FA lysis buffer and sonicated using the Qsonica Q800R at 100% amplitude with 10-s ON and 15-s OFF cycles for a total sonication time of 30 min. The arising chromatin solution was recovered by centrifugation at 14,000 rpm for 30 min at 4°C and stored at  $-80^{\circ}\text{C}$  until use. Chromatin size ( $\sim$ 100 to 300 bp) and quality were checked on a 2% agarose gel. PolII immunoprecipitation was performed by mixing 50  $\mu$ l of chromatin extract with 450  $\mu$ l of FA lysis buffer and 2  $\mu$ l of anti-RNA polymerase II subunit antibodies (clone 3E8; Millipore) for 1.5 h, followed by incubating the mixture with  $\sim$ 15  $\mu$ l packed protein A Sepharose (GE Healthcare) for another 1.5 h at room temperature on an end-to-end rotator. Subsequently, protein A Sepharose matrix was transferred to a Corning Costar SpinX centrifuge tube filter and washed. Immunoprecipitated chromatin DNA was de-cross-linked at 65°C overnight and then was purified using a Qiagen PCR cleanup purification column. Library preparation was carried out using an NEBNext Ultra II library prep kit (Illumina; catalog no. E7645L) according to the manufacturer's protocol and barcoded adaptors as described in the work of Wong et al. (76). Libraries were checked and quantified using a DNA High Sensitivity Bioanalyzer assay (Agilent; catalog no. XF06BK50), mixed in equal molar ratio, and sequenced using the Illumina HiSeq2500 platform at the Genomics and Single Cells Analysis Core facility at the University of Macau.

Raw sequencing reads were mapped to the *A. fumigatus* strain Af293 reference genome (AspGD version s03-m05-r06) using Bowtie2 (v2.3.5) (77). PolII binding levels were measured by counting number of reads over coding regions and normalizing as FPKM (fragments per kilobase per million) scores. For ChIP-Seq signal data visualization purpose, aligned reads were extended to 200 bp using the 'macs2 pileup' command and scaled to 1 million mapped reads using the 'macs2 bdgopt' command from the MACS2 (v2.1.1) tool (78). UCSC Kent Utils programs (79) 'bedSort' and 'bedGraphToBigWig' were used to generate BigWig files, which were visualized in Integrative Genomics Viewer (v2.5.3) (80).

**Cell wall polysaccharide extraction and sugar quantification.** Fungal cell wall polysaccharides were extracted from 100 mg dry-frozen biomass as described previously using TCA (trichloroacetic acid) hydrolysis (81). Total carbohydrates were estimated using the phenol sulfuric method as described by Masuko et al. (82). Released sugars from hydrolysis were subsequently analyzed by high-performance liquid chromatography (HPLC) using a YoungLin YL9100 series system (YoungLin, Anyang, South Korea) equipped with a YL9170 series refractive index (RI) detector at 40°C. Samples were loaded in a Rezex ROA (Phenomenex, USA) column (300  $\times$  7.8 mm) at 85°C and eluted with 0.05 M sulfuric acid at a flow rate of 0.5 ml/min. All sugar concentrations were expressed in millimolar (mM) using a correspondent standard curve.

**Staining for dectin-1, chitin, and other cell surface carbohydrates.** Cell wall surface polysaccharide staining was performed as described previously (83, 84). Briefly, strains were grown from  $2.5 \times 10^3$  spores in 200  $\mu$ l of MM for 16 h at 37°C before the culture medium was removed and germlings were UV irradiated (600,000  $\mu$ J). Hyphal germlings were subsequently washed with  $1 \times$  phosphate-buffered saline (PBS), and 200  $\mu$ l of a blocking solution (2% [wt/vol] goat serum, 1% [wt/vol] bovine serum albumin [BSA], 0.1% [vol/vol] Triton X-100, 0.05% [vol/vol] Tween 20, 0.05% [vol/vol] sodium azide, and 0.01 M PBS) was added. Samples were incubated for 30 min at room temperature (RT). For dectin staining, 0.2  $\mu$ g/ml of Fc-h-dectin-hFc was added to the UV-irradiated germlings and incubated for 1 h at RT, followed by the addition of 1:1,000 DyLight 594-conjugated, goat anti-human IgG1 for 1 h at RT. Germlings were washed with PBS, and fluorescence was read at 587-nm excitation and 615-nm emission. For chitin staining, 200  $\mu$ l of a PBS solution with 10  $\mu$ g/ml of calcofluor white (CFW) was added to the UV-irradiated germlings, which were incubated for 5 min at RT and washed three times with PBS before fluorescence was read at 380-nm excitation and 450-nm emission. For galactosaminogalactan (GAG), GlcN (glucosamine), and mannose staining, 200  $\mu$ l of PBS supplemented with 0.1 mg/ml of either soybean agglutinin-fluorescein isothiocyanate (SBA-FITC) (*Glycine max* soybean lectin SBA-FITC; Bioworld; catalog no. 21761024-2), wheat germ agglutinin (WGA) (lectin-FITC L4895; Sigma), or concanavalin A (ConA; C7642; Sigma) was added to the UV-irradiated germlings for 1 h at RT. Germlings were washed with PBS, and fluorescence was read at 492-nm excitation and 517-nm emission. All experiments were performed using 12 repetitions, and fluorescence was read in a microtiter plate reader (SpectraMax i3; Molecular Devices).

**Transmission electron microscopy (TEM) analysis of cell wall.** Strains were grown statically from  $1 \times 10^7$  conidia at 37°C in MM for 24 h. Mycelia were harvested and immediately fixed in 0.1 M sodium phosphate buffer (pH 7.4) containing 2.5% (vol/vol) glutaraldehyde and 2% (wt/vol) paraformaldehyde for 24 h at 4°C. Samples were encapsulated in agar (2%, wt/vol) and subjected to fixation (1% OsO<sub>4</sub>), contrasting (1% uranyl acetate), ethanol dehydration, and a two-step infiltration process with Spurr resin (Electron Microscopy Sciences) of 16 h and 3 h at RT. Additional infiltration was provided under vacuum at RT before embedment in BEEM capsules (Electron Microscopy Sciences) and polymerization at 60°C for 72 h. Semithin (0.5- $\mu$ m) survey sections were stained with toluidine blue to identify the areas of best cell density. Ultrathin sections (60 nm) were prepared and stained again with uranyl acetate (1%) and lead citrate (2%). Transmission electron microscopy (TEM) images were obtained using a Philips CM-120 electron microscope at an acceleration voltage of 120 kV using a MegaView3 camera and iTEM 5.0 software (Olympus Soft Imaging Solutions GmbH). Cell wall thicknesses of 100 sections of different germlings were measured at  $\times$ 23,500 magnification, and images were analyzed with the ImageJ software (85). Statistical differences were evaluated by using one-way analysis of variance (ANOVA) and Tukey's *post hoc* test.

**Ethics statement.** Animal experiments were performed in strict accordance with Brazilian Federal Law 11794, establishing procedures for the scientific use of animals in strict accordance with the

principles outlined by the Brazilian College of Animal Experimentation (CONCEA), and the state law establishing the animal protection code of the State of São Paulo. All protocols adopted in this study were approved by the local ethics committee for animal experiments from the University of São Paulo, Campus of Ribeirão Preto (permit number 08.1.1277.53.6; Studies on the interaction of *Aspergillus fumigatus* with animals). All efforts were made to minimize suffering. All stressed animals were sacrificed by cervical dislocation after intraperitoneal (i.p.) injection of ketamine and xylazine.

**Murine model of pulmonary aspergillosis, lung histopathology, and fungal burden.** Outbred female mice (BALB/c strain; body weight, 20 to 22 g) were housed in vented cages containing five animals. Mice were immunosuppressed with cyclophosphamide (150 mg per kg of body weight), which was administered intraperitoneally on days  $-4$ ,  $-1$ , and  $2$  prior to and after infection. Hydrocortisonacetate (200 mg/kg body weight) was injected subcutaneously on day  $-3$ . *A. fumigatus* strains were grown on YAG for 2 days prior to infection. Fresh conidia were harvested in PBS and filtered through Miracloth (Calbiochem). Conidial suspensions were spun for 5 min at  $3,000 \times g$ , washed three times with PBS, counted using a hemocytometer, and resuspended at a concentration of  $5.0 \times 10^6$  conidia/ml. The viability of the administered inoculum was determined by incubating a serial dilution of the conidia on YAG medium, at  $37^\circ\text{C}$ . Mice were anesthetized by halothane inhalation and infected by intranasal instillation of  $1.0 \times 10^5$  conidia in 20 ml of PBS. As a negative control, a group of five mice received PBS only. Mice were weighed every 24 h from the day of infection and visually inspected twice daily. The statistical significance of the comparative survival values was calculated using log rank analysis and the Prism statistical analysis package (GraphPad Software Inc.).

To investigate fungal burden in murine lungs, mice were immunosuppressed with cyclophosphamide (150 mg/kg of body weight), which was administered intraperitoneally on days  $-4$  and  $-1$ , while hydrocortisonacetate was injected subcutaneously (200 mg/kg) on day  $-3$ . Five mice per group were intranasally inoculated with  $1 \times 10^6$  conidia/20 ml of suspension. A higher inoculum, in comparison to the survival experiments, was used to increase fungal DNA detection. Animals were sacrificed 72 h post-infection, and the lungs were harvested and immediately frozen in liquid nitrogen. Samples were homogenized by vortexing with glass beads for 10 min, and DNA was extracted via the phenol-chloroform method. DNA quantity and quality were assessed using a NanoDrop 2000 spectrophotometer (Thermo Scientific). At least 500 mg of total DNA from each sample was used for quantitative real-time PCRs. Specific primers were used to amplify the 18S rRNA region of *A. fumigatus* and an intronic region of mouse GAPDH (glyceraldehyde-3-phosphate dehydrogenase) (see Table S6 at <https://doi.org/10.6084/m9.figshare.12931754.v3>). Six-point standard curves were calculated using serial dilutions of gDNA from all the *A. fumigatus* strains used and the uninfected mouse lung. Fungal and mouse DNA quantities were obtained from the threshold cycle ( $C_T$ ) values from an appropriate standard curve (74). Fungal burden was determined as the ratio between picograms of fungal DNA and micrograms of mouse DNA.

For histopathology studies, the animals were also sacrificed 72 h postinfection and lungs were removed and fixed for 24 h in 3.7% formaldehyde-PBS. Samples were washed several times in 70% alcohol before dehydration in a series of alcohol solutions of increasing concentrations. Finally, samples were diaphanized in xylol and embedded in paraffin. For each sample, sequential 5-mm-thick sections were collected on glass slides and stained with Grocott's methenamine silver (GMS) or hematoxylin and eosin (HE) stain following standard protocols. Briefly, sections were deparaffinized, oxidized with 4% chromic acid, stained with methenamine silver solution, and counterstained with picric acid. For HE staining, sections were deparaffinized and stained first with hematoxylin and then with eosin. All stained slides were immediately washed, preserved with mounting medium, and sealed with a coverslip. Microscopic analyses were done using an AxioPlan 2 imaging microscope (Zeiss) at the stated magnifications under bright-field conditions.

***A. fumigatus* infection in immunocompetent mice.** Eight- to 12-week-old male C57BL/6 WT mice were obtained from the specific-pathogen-free Isogenic Breeding Unit of the Department of Immunology, Institute of Biomedical Sciences, University of São Paulo. Mice were anesthetized and submitted to intratracheal (i.t.) infection as previously described (86) and further adapted to the *A. fumigatus* infection model (30, 87). Briefly, after intraperitoneal (i.p.) injection of ketamine and xylazine, animals were inoculated with  $5 \times 10^7$  CEA17 wild-type,  $\Delta nsdC$ , or  $\Delta nsdC::nsdC^+$  conidia, contained in  $75 \mu\text{l}$  of PBS, by surgical i.t. inoculation, which allowed dispensing of the fungal cells directly into the lungs.

**Assessment of leukocyte subpopulations and flow cytometric analysis.** Lungs from *A. fumigatus*-inoculated mice were collected after 3 days of exposure to the microbe. To assess the leukocyte subpopulations, the lungs were removed and digested enzymatically for 40 min with collagenase (2 mg/ml) in RPMI culture medium (Sigma). Total lung leukocyte numbers were assessed with trypan blue, and viability was always  $>95\%$ . For cell surface staining, leukocytes were washed and suspended at  $1 \times 10^6$  cells/ml in staining buffer (PBS, 2% fetal calf serum, and 0.1%  $\text{NaN}_3$ ). Fc receptors were blocked by the addition of unlabeled anti-CD16/32 (eBioscience). Leukocytes were then stained in the dark for 25 min at  $4^\circ\text{C}$  with the optimal dilution of each monoclonal antibody. The following were added to total leukocytes, neutrophils, and macrophages: anti-CD45, CD11b, Ly6G, Ly6C, F4/80, CD40, MHC-II, and CD86 (eBioscience or BioLegend). Cells were washed twice with staining buffer, before being fixed with 2% paraformaldehyde (PFA; Sigma). A minimum of 100,000 events was acquired on a FACSLyric flow cytometer (BD Biosciences) using the FACSDiva software (BD Biosciences). Total leukocytes, macrophages, and neutrophils were gated as judged from forward and side light scatter. The cell surface expression of leukocyte markers was analyzed using the FlowJo software (Tree Star).

**Bone marrow-derived macrophage (BMDM) preparation, phagocytosis, and killing assay.** The BMDM preparation was performed according to the work of Marim et al. (88) with some modifications. BMDMs were prepared from C57BL/6 adult mouse femurs and tibias. These cells were cultured for 6 days in RPMI 1640 medium supplemented with 20% fetal cow serum (FCS) and 30% L-929 cell-

conditioned medium. Nonadherent cells were removed, and the adherent cells (majority macrophages) were removed and washed twice with cold PBS. Cell concentration was determined using a Neubauer chamber. The phagocytic assay was performed as previously described (89) with slight modifications. In 24-well microplates at 37°C with 5% CO<sub>2</sub>, 1 ml of RPMI-FCS containing 1 × 10<sup>5</sup> conidia (1:5 macrophage/conidium ratio) was added and incubated for 90 min. The supernatant was removed, and 0.5 ml of 3.7% formaldehyde-PBS was added. The samples were washed with ultrapure water and incubated for 20 min with 495 μl of water and 5 μl of CFW (10 mg/ml). Samples were washed and mounted on slides with 50% glycerol. Images were then acquired on an Eclipse E800 fluorescence microscope (Nikon Instruments), and the phagocytosis index was calculated counting at least 100 conidia per sample. The experiments were repeated in triplicate. To assess conidial killing, the phagocytic cells were obtained as described above. Subsequently, 1 × 10<sup>5</sup> conidia (1:5 macrophage/conidium ratio) were incubated at 37°C with 5% CO<sub>2</sub> for 4 h. As positive control, conidia without BMDMs were used. The 24-well microplates were centrifuged for 10 min at 3,500 rpm, and the culture supernatant was removed. Then, 100 μl of 1% Triton X-100 was added. After 10 min at room temperature, samples were removed from the microplate, washed three times with sterile distilled water, and serially diluted in PBS. The dilutions were plated and incubated at 37°C for 48 h. The percentage of conidial killing was calculated by the measurement of CFU numbers carried out after macrophage lysis, comparing CFU numbers from samples incubated with macrophages to CFU numbers from those incubated without macrophages. The experiments were repeated three times, each performed in triplicate.

**Data availability.** The transcriptional profiling for *ΔnsdC* was investigated using ChIP of RNA polymerase II coupled to DNA sequencing. Short reads were deposited in the NCBI, under GEO accession number [GSE148557](https://www.ncbi.nlm.nih.gov/geo/query/acc.cgi?acc=GSE148557).

## ACKNOWLEDGMENTS

We thank São Paulo Research Foundation (FAPESP) grant numbers 2016/07870-9 (G.H.G.), 2018/00715-3 (C.V.), 2016/12948-7 (P.A.D.C.), 2016/22062-6 (J.C.), 2016/21392-2 (L.P.S.), 2019/10097-8 (F.V.L.), and 2017/07536-4 (A.C.C.) and Conselho Nacional de Desenvolvimento Científico e Tecnológico (CNPq) (G.H.G.), both from Brazil, for financial support. K.H.W. also acknowledges the support from the Research Services and Knowledge Transfer Office (MYRG2018-00017-FHS and MYRG2019-00099-FHS) of the University of Macau and the Collaborative Research Fund Equipment Grant (C5012-15E) from the Research Grant Council, Hong Kong Government. P.S.D. thanks the Natural Environment Research Council (UK) for support (NE/P000916/1).

## REFERENCES

- Kontoyiannis DP, Bodey GP. 2002. Invasive aspergillosis in 2002: an update. *Eur J Clin Microbiol Infect Dis* 21:161–172. <https://doi.org/10.1007/s10096-002-0699-z>.
- Brown GD, Denning DW, Gow NA, Levitz SM, Netea MG, White TC. 2012. Hidden killers: human fungal infections. *Sci Transl Med* 4:165rv13. <https://doi.org/10.1126/scitranslmed.3004404>.
- Bongomin F, Gago S, Oladele RO, Denning DW. 2017. Global and multinational prevalence of fungal diseases—estimate precision. *J Fungi* 3:57. <https://doi.org/10.3390/jof3040057>.
- Gregg KS, Kauffman CA. 2015. Invasive aspergillosis: epidemiology, clinical aspects, and treatment. *Semin Respir Crit Care Med* 36:662–672. <https://doi.org/10.1055/s-0035-1562893>.
- Park HS, Yu JH. 2016. Developmental regulators in *Aspergillus fumigatus*. *J Microbiol* 54:223–231. <https://doi.org/10.1007/s12275-016-5619-5>.
- Ojeda-López M, Chen W, Eagle CE, Gutiérrez G, Jia WL, Swilaiman SS, Huang Z, Park HS, Yu JH, Cánovas D, Dyer PS. 2018. Evolution of asexual and sexual reproduction in the aspergilli. *Stud Mycol* 91:37–59. <https://doi.org/10.1016/j.simyco.2018.10.002>.
- Geiser DM, Klich MA, Frisvad JC, Peterson SW, Varga J, Samson RA. 2007. The current status of species recognition and identification in *Aspergillus*. *Stud Mycol* 59:1–10. <https://doi.org/10.3114/sim.2007.59.01>.
- Dyer PS, O’Gorman CM. 2011. A fungal sexual revolution: *Aspergillus* and *Penicillium* show the way. *Curr Opin Microbiol* 14:649–654. <https://doi.org/10.1016/j.mib.2011.10.001>.
- Adams TH, Boylan MT, Timberlake WE. 1988. brIA is necessary and sufficient to direct conidiophore development in *Aspergillus nidulans*. *Cell* 54:353–362. [https://doi.org/10.1016/0092-8674\(88\)90198-5](https://doi.org/10.1016/0092-8674(88)90198-5).
- Andrianopoulos A, Timberlake WE. 1994. The *Aspergillus nidulans* *abaA* gene encodes a transcriptional activator that acts as a genetic switch to control development. *Mol Cell Biol* 14:2503–2515. <https://doi.org/10.1128/mcb.14.4.2503>.
- Mah JH, Yu JH. 2006. Upstream and downstream regulation of asexual development in *Aspergillus fumigatus*. *Eukaryot Cell* 5:1585–1595. <https://doi.org/10.1128/EC.00192-06>.
- Tao L, Yu JH. 2011. AbaA and WetA govern distinct stages of *Aspergillus fumigatus* development. *Microbiology (Reading)* 157:313–326. <https://doi.org/10.1099/mic.0.044271-0>.
- Alkhayyat F, Chang Kim S, Yu JH. 2015. Genetic control of asexual development in *Aspergillus fumigatus*. *Adv Appl Microbiol* 90:93–107. <https://doi.org/10.1016/bs.aambs.2014.09.004>.
- Park HS, Bayram O, Braus GH, Kim SC, Yu JH. 2012. Characterization of the velvet regulators in *Aspergillus fumigatus*. *Mol Microbiol* 86:937–953. <https://doi.org/10.1111/mmi.12032>.
- Xiao P, Shin KS, Wang T, Yu JH. 2010. *Aspergillus fumigatus* *flbB* encodes two basic leucine zipper domain (bZIP) proteins required for proper asexual development and gliotoxin production. *Eukaryot Cell* 9:1711–1723. <https://doi.org/10.1128/EC.00198-10>.
- Shin KS, Kwon NJ, Yu JH. 2009. Gbetagamma-mediated growth and developmental control in *Aspergillus fumigatus*. *Curr Genet* 55:631–641. <https://doi.org/10.1007/s00294-009-0276-4>.
- Kwon NJ, Park HS, Jung S, Kim SC, Yu JH. 2012. The putative guanine nucleotide exchange factor RicA mediates upstream signaling for growth and development in *Aspergillus*. *Eukaryot Cell* 11:1399–1412. <https://doi.org/10.1128/EC.00255-12>.
- Manfiolli AO, Siqueira FS, Dos Reis TF, Van Dijk P, Schrevels S, Hoefgen S, Föge M, Straßburger M, de Assis LJ, Heinekamp T, Rocha MC, Janevska S, Brakhage AA, Malavazi I, Goldman GH, Valiante V. 2019. Mitogen-activated protein kinase cross-talk interaction modulates the production of melanins in *Aspergillus fumigatus*. *mBio* 10:e00215-19. <https://doi.org/10.1128/mBio.00215-19>.
- Varga J, Toth B. 2003. Genetic variability and reproductive mode of *Aspergillus fumigatus*. *Infect Genet Evol* 3:3–17. [https://doi.org/10.1016/s1567-1348\(02\)00156-9](https://doi.org/10.1016/s1567-1348(02)00156-9).
- Paoletti M, Rydholm C, Schwier EU, Anderson MJ, Szakacs G, Lutzoni F,

- Debeaupuis JP, Latgé JP, Denning DW, Dyer PS. 2005. Evidence for sexual-ity in the opportunistic fungal pathogen *Aspergillus fumigatus*. *Curr Biol* 15:1242–1248. <https://doi.org/10.1016/j.cub.2005.05.045>.
21. Pringle A, Baker DM, Platt JL, Wares JP, Latge JP, Taylor JW. 2005. Cryptic speciation in the cosmopolitan and clonal human pathogenic fungus *Aspergillus fumigatus*. *Evolution* 59:1886–1899. <https://doi.org/10.1111/j.0014-3820.2005.tb01059.x>.
  22. O’Gorman CM, Fuller H, Dyer PS. 2009. Discovery of a sexual cycle in the opportunistic fungal pathogen *Aspergillus fumigatus*. *Nature* 457:471–474. <https://doi.org/10.1038/nature07528>.
  23. Sugui JA, Losada L, Wang W, Varga J, Ngamskulrungrroj P, Abu-Asab M, Chang YC, O’Gorman CM, Wickes BL, Nierman WC, Dyer PS, Kwon-Chung KJ. 2011. Identification and characterization of an *Aspergillus fumigatus* “super-mater” pair. *mBio* 2:e00234-11. <https://doi.org/10.1128/mBio.00234-11>.
  24. Ashton GD, Dyer PS. 2019. Culturing and mating of *Aspergillus fumigatus*. *Curr Protoc Microbiol* 54:e87. <https://doi.org/10.1002/cpmc.87>.
  25. Szweczyk E, Krappmann S. 2010. Conserved regulators of mating are essential for *Aspergillus fumigatus* cleistothecium formation. *Eukaryot Cell* 9:774–783. <https://doi.org/10.1128/EC.00375-09>.
  26. Dyer PS, Kuck U. 2017. Sex and the imperfect fungi. *Microbiol Spectr* 5:FUNK-0043-2017. <https://doi.org/10.1128/microbiolspec.FUNK-0043-2017>.
  27. Dyer PS, O’Gorman CM. 2012. Sexual development and cryptic sexuality in fungi: insights from *Aspergillus* species. *FEMS Microbiol Rev* 36:165–192. <https://doi.org/10.1111/j.1574-6976.2011.00308.x>.
  28. Paoletti M, Seymour FA, Alcocer MJC, Kaur N, Calvo AM, Archer DB, Dyer PS. 2007. Mating type and the genetic basis of self-fertility in the model fungus *Aspergillus nidulans*. *Curr Biol* 17:1384–1389. <https://doi.org/10.1016/j.cub.2007.07.012>.
  29. Kim HR, Chae KS, Han KH, Han DM. 2009. The nsdC gene encoding a putative C2H2-type transcription factor is a key activator of sexual development in *Aspergillus nidulans*. *Genetics* 182:771–783. <https://doi.org/10.1534/genetics.109.101667>.
  30. de Castro PA, Colabardini AC, Manfioli AO, Chiaratto J, Silva LP, Mattos EC, Palmisano G, Almeida F, Persinoti GF, Ries LNA, Mellado L, Rocha MC, Bromley M, Silva RN, de Souza GS, Loures FV, Malavazi I, Brown NA, Goldman GH. 2019. *Aspergillus fumigatus* calcium-responsive transcription factors regulate cell wall architecture promoting stress tolerance, virulence and caspofungin resistance. *PLoS Genet* 15:e1008551. <https://doi.org/10.1371/journal.pgen.1008551>.
  31. Han Z, Tian L, Pecot T, Huang T, Machiraju R, Huang K. 2012. A signal processing approach for enriched region detection in RNA polymerase II ChIP-seq data. *BMC Bioinformatics* 13(Suppl 2):S2. <https://doi.org/10.1186/1471-2105-13-S2-S2>.
  32. Mokry M, Hatzis P, Schuijers J, Lansu N, Ruzius FP, Clevers H, Cuppen E. 2012. Integrated genome-wide analysis of transcription factor occupancy, RNA polymerase II binding and steady-state RNA levels identify differentially regulated functional gene classes. *Nucleic Acids Res* 40:148–158. <https://doi.org/10.1093/nar/gkr720>.
  33. Vienken K, Fischer R. 2006. The Zn(II)2Cys6 putative transcription factor NosA controls fruiting body formation in *Aspergillus nidulans*. *Mol Microbiol* 61:544–554. <https://doi.org/10.1111/j.1365-2958.2006.05257.x>.
  34. Busch S, Schwier EU, Nahlik K, Bayram O, Helmstaedt K, Draht OW, Krappmann O, Valerius O, Lipscomb WN, Braus G. 2007. An eight-subunit COP9 signalosome with an intact JAMM motif is required for fungal fruit body formation. *Proc Natl Acad Sci U S A* 104:8089–8094. <https://doi.org/10.1073/pnas.0702108104>.
  35. Alkahyyat F, Ni M, Kim SC, Yu JH. 2015. The WOPR domain protein OsaA orchestrates development in *Aspergillus nidulans*. *PLoS One* 10:e0137554. <https://doi.org/10.1371/journal.pone.0137554>.
  36. Lee MK, Kwon NJ, Lee IS, Jung S, Kim SC, Yu JH. 2016. Negative regulation and developmental competence in *Aspergillus*. *Sci Rep* 6:28874. <https://doi.org/10.1038/srep28874>.
  37. Bayram O, Sari F, Braus GH, Irmiger S. 2009. The protein kinase ImeB is required for light-mediated inhibition of sexual development and for mycotoxin production in *Aspergillus nidulans*. *Mol Microbiol* 71:1278–1295. <https://doi.org/10.1111/j.1365-2958.2009.06606.x>.
  38. Wieser J, Adams TH. 1995. flbD encodes a Myb-like DNA-binding protein that coordinates initiation of *Aspergillus nidulans* conidiophore development. *Genes Dev* 9:491–502. <https://doi.org/10.1101/gad.9.4.491>.
  39. Seo JA, Guan Y, Yu JH. 2003. Suppressor mutations bypass the requirement of fluG for asexual sporulation and sterigmatocystin production in *Aspergillus nidulans*. *Genetics* 165:1083–1093.
  40. Wieser J, Lee BN, Fondon J, III, Adams TH. 1994. Genetic requirements for initiating asexual development in *Aspergillus nidulans*. *Curr Genet* 27:62–69. <https://doi.org/10.1007/BF00326580>.
  41. Sarikaya-Bayram O, Bayram O, Feussner K, Kim JH, Kim HS, Kaefer A, Feussner I, Chae KS, Han DM, Han KH, Braus GH. 2014. Membrane-bound methyltransferase complex VapA-VipC-VapB guides epigenetic control of fungal development. *Dev Cell* 29:406–420. <https://doi.org/10.1016/j.devcel.2014.03.020>.
  42. Balloy V, Chignard M. 2009. The innate immune response to *Aspergillus fumigatus*. *Microbes Infect* 11:919–927. <https://doi.org/10.1016/j.micinf.2009.07.002>.
  43. Han DM, Han YJ, Kim JH, Jahng KY, Chung YS, Chung JH, Chae KS. 1994. Isolation and characterization of NSD mutants in *Aspergillus nidulans*. *Korean J Mycol* 22:1–7.
  44. Han KH, Han DM. 2010. Genetics and genomics of sexual development of *Aspergillus nidulans*, p 115–137. In Machida M, Gomi K (ed), *Aspergillus molecular biology and genomics*. Caister Academic Press, Norfolk, United Kingdom.
  45. Han KH, Han KY, Yu JH, Chae K, Jahng KY, Han DM. 2001. The nsdD gene encodes a putative GATA-type transcription factor necessary for sexual development of *Aspergillus nidulans*. *Mol Microbiol* 41:299–309. <https://doi.org/10.1046/j.1365-2958.2001.02472.x>.
  46. Caplan T, Polvi EJ, Xie JL, Buckhalter S, Leach MD, Robbins N, Cowen LE. 2018. Functional genomic screening reveals core modulators of echinocandin stress responses in *Candida albicans*. *Cell Rep* 23:2292–2298. <https://doi.org/10.1016/j.celrep.2018.04.084>.
  47. Damveld RA, Franken A, Arentshorst M, Punt PJ, Klis FM, van den Hondel CA, Ram AFJ. 2008. A novel screening method for cell wall mutants in *Aspergillus niger* identifies UDP-galactopyranose mutase as an important protein in fungal cell wall biosynthesis. *Genetics* 178:873–881. <https://doi.org/10.1534/genetics.107.073148>.
  48. Macdonald D, Thomson DD, Johns A, Contreras Valenzuela A, Gillesen JM, Lord KM, Bowyer P, Denning DW, Read ND, Bromley MJ. 2018. Inducible cell fusion permits use of competitive fitness profiling in the human pathogenic fungus *Aspergillus fumigatus*. *Antimicrob Agents Chemother* 63:e01615-18. <https://doi.org/10.1128/AAC.01615-18>.
  49. Ries LNA, Rocha MC, de Castro PA, Silva-Rocha R, Silva RN, Freitas FZ, de Assis LJ, Bertolini MC, Malavazi I, Goldman GH. 2017. The *Aspergillus fumigatus* CrzA transcription factor activates chitin synthase gene expression during the caspofungin paradoxical effect. *mBio* 8:e00705-17. <https://doi.org/10.1128/mBio.00705-17>.
  50. Braus GH, Krappmann S, Eckert SE. 2002. Sexual development in ascomycetes. Fruit body formation of *Aspergillus nidulans*, p 215–244. In Osiewacz HD (ed), *Molecular biology of fungal development*. Marcel Dekker, New York, NY.
  51. Sohn KT, Yoon KS. 2002. Ultrastructural study on the cleistothecium development in *Aspergillus nidulans*. *Mycobiology* 30:117–127. <https://doi.org/10.4489/MYCO.2002.30.3.117>.
  52. Cary JW, Harris-Coward PY, Ehrlich KC, Mack BM, Kale SP, Larey C, Calvo AM. 2012. NsdC and NsdD affect *Aspergillus flavus* morphogenesis and aflatoxin production. *Eukaryot Cell* 11:1104–1111. <https://doi.org/10.1128/EC.00069-12>.
  53. Son H, Seo Y-S, Min K, Park AR, Lee J, Jin J-M, Lin Y, Cao P, Hong S-Y, Kim E-K, Lee S-H, Cho A, Lee S, Kim M-G, Kim Y, Kim J-E, Kim J-C, Choi GJ, Yun S-H, Lim JY, Kim M, Lee Y-H, Choi Y-D, Lee Y-W. 2011. A phenome-based functional analysis of transcription factors in the cereal head blight fungus, *Fusarium graminearum*. *PLoS Pathog* 7:e1002310. <https://doi.org/10.1371/journal.ppat.1002310>.
  54. Teichert I, Nowrousian M, Poggeker S, Kuck U. 2014. The filamentous fungus *Sordaria macrospora* as a genetic model to study fruiting body development. *Adv Genet* 87:199–244. <https://doi.org/10.1016/B978-0-12-800149-3.00004-4>.
  55. Yu Y, Amich J, Will C, Eagle CE, Dyer PS, Krappmann S. 2017. The novel *Aspergillus fumigatus* MAT1-2-4 mating-type gene is required for mating and cleistothecia formation. *Fungal Genet Biol* 108:1–12. <https://doi.org/10.1016/j.fgb.2017.09.001>.
  56. Yu JH. 2010. Regulation of development in *Aspergillus nidulans* and *Aspergillus fumigatus*. *Mycobiology* 38:229–237. <https://doi.org/10.4489/MYCO.2010.38.4.229>.
  57. Kang JY, Chun J, Jun S-C, Han D-M, Chae K-S, Jahng KY. 2013. The MpkB MAP kinase plays a role in autolysis and conidiation of *Aspergillus nidulans*. *Fungal Genet Biol* 61:42–49. <https://doi.org/10.1016/j.fgb.2013.09.010>.
  58. van de Veerdonk FL, Gresnigt MS, Romani L, Netea MG, Latge JP. 2017.

- Aspergillus fumigatus morphology and dynamic host interactions. *Nat Rev Microbiol* 15:661–674. <https://doi.org/10.1038/nrmicro.2017.90>.
59. Cramer RA, Jr, Perfect BZ, Pinchai N, Park S, Perlin DS, Asfaw YG, Heitman J, Perfect JR, Steinbach WJ. 2008. Calcineurin target CrzA regulates conidial germination, hyphal growth, and pathogenesis of *Aspergillus fumigatus*. *Eukaryot Cell* 7:1085–1097. <https://doi.org/10.1128/EC.00086-08>.
  60. Soriani FM, Malavazi I, da Silva Ferreira ME, Savoldi M, Von Zeska Kress MR, Souza Goldman MH, Löss O, Bignell E, Goldman GH. 2008. Functional characterization of the *Aspergillus fumigatus* CRZ1 homologue, CrzA. *Mol Microbiol* 67:1274–1291. <https://doi.org/10.1111/j.1365-2958.2008.06122.x>.
  61. Soriani FM, Malavazi I, Savoldi M, Espeso E, Dinamarco TM, Bernardes LA, Ferreira M, Goldman MHS, Goldman GH. 2010. Identification of possible targets of the *Aspergillus fumigatus* CRZ1 homologue, CrzA. *BMC Microbiol* 10:12. <https://doi.org/10.1186/1471-2180-10-12>.
  62. de Castro PA, Chen C, de Almeida RS, Freitas FZ, Bertolini MC, Morais ER, Brown NA, Ramalho LN, Hagiwara D, Mitchell TK, Goldman GH. 2014. ChIP-seq reveals a role for CrzA in the *Aspergillus fumigatus* high-osmolarity glycerol response (HOG) signalling pathway. *Mol Microbiol* 94:655–674. <https://doi.org/10.1111/mmi.12785>.
  63. Thewes S. 2014. Calcineurin-Crz1 signaling in lower eukaryotes. *Eukaryot Cell* 13:694–705. <https://doi.org/10.1128/EC.00038-14>.
  64. Espeso EA. 2016. The CrZy calcium cycle. *Adv Exp Med Biol* 892:169–186. [https://doi.org/10.1007/978-3-319-25304-6\\_7](https://doi.org/10.1007/978-3-319-25304-6_7).
  65. Brown NA, Goldman GH. 2016. The contribution of *Aspergillus fumigatus* stress responses to virulence and antifungal resistance. *J Microbiol* 54:243–253. <https://doi.org/10.1007/s12275-016-5510-4>.
  66. Rocha MC, Fabri JH, Franco de Godoy K, Alves de Castro P, Hori JI, Ferreira da Cunha A, Arentshorst M, Ram AF, van den Hondel CA, Goldman GH, Malavazi I. 2016. *Aspergillus fumigatus* MADS-box transcription factor rlmA is required for regulation of the cell wall integrity and virulence. *G3 (Bethesda)* 6:2983–3002. <https://doi.org/10.1534/g3.116.031112>.
  67. Latgé J-P, Chamilos G. 2019. *Aspergillus fumigatus* and aspergillosis in 2019. *Clin Microbiol Rev* 33:e00140-18. <https://doi.org/10.1128/CMR.00140-18>.
  68. Li S, Bao D, Yuen G, Harris SD, Calvo AM. 2007. basA regulates cell wall organization and asexual/sexual sporulation ratio in *Aspergillus nidulans*. *Genetics* 176:243–253. <https://doi.org/10.1534/genetics.106.068239>.
  69. Gastebois A, Clavaud C, Aimaniananda V, Latgé JP. 2009. *Aspergillus fumigatus*: cell wall polysaccharides, their biosynthesis and organization. *Future Microbiol* 4:583–595. <https://doi.org/10.2217/fmb.09.29>.
  70. Sales-Campos H, Tonani L, Cardoso CR, Kress MR. 2013. The immune interplay between the host and the pathogen in *Aspergillus fumigatus* lung infection. *Biomed Res Int* 2013:693023. <https://doi.org/10.1155/2013/693023>.
  71. Kafer E. 1977. Meiotic and mitotic recombination in *Aspergillus* and its chromosomal aberrations. *Adv Genet* 19:33–131. [https://doi.org/10.1016/S0065-2660\(08\)60245-X](https://doi.org/10.1016/S0065-2660(08)60245-X).
  72. Brock M, Jouvion G, Droin-Bergère S, Dussurget O, Nicola MA, Ibrahim-Granet O. 2008. Bioluminescent *Aspergillus fumigatus*, a new tool for drug efficiency testing and in vivo monitoring of invasive aspergillosis. *Appl Environ Microbiol* 74:7023–7035. <https://doi.org/10.1128/AEM.01288-08>.
  73. Geib E, Gressler M, Viedernikova I, Hillmann F, Jacobsen ID, Nietzsche S, Hertweck C, Brock M. 2016. A non-canonical melanin biosynthesis pathway protects *Aspergillus terreus* conidia from environmental stress. *Cell Chem Biol* 23:587–597. <https://doi.org/10.1016/j.chembiol.2016.03.014>.
  74. Semighini CP, Marins M, Goldman MH, Goldman GH. 2002. Quantitative analysis of the relative transcript levels of ABC transporter Atr genes in *Aspergillus nidulans* by real-time reverse transcription-PCR assay. *Appl Environ Microbiol* 68:1351–1357. <https://doi.org/10.1128/aem.68.3.1351-1357.2002>.
  75. Suzuki Y, Murray SL, Wong KH, Davis MA, Hynes MJ. 2012. Reprogramming of carbon metabolism by the transcriptional activators AcuK and AcuM in *Aspergillus nidulans*. *Mol Microbiol* 84:942–964. <https://doi.org/10.1111/j.1365-2958.2012.08067.x>.
  76. Wong KH, Jin Y, Moqtaderi Z. 2013. Multiplex Illumina sequencing using DNA barcoding. *Curr Protocol Mol Biol Chapter 7:Unit 7.11*. <https://doi.org/10.1002/0471142727.mb0711s101>.
  77. Langmead B, Salzberg SL. 2012. Fast gapped-read alignment with Bowtie2. *Nat Methods* 9:357–359. <https://doi.org/10.1038/nmeth.1923>.
  78. Zhang Y, Liu T, Meyer CA, Eeckhoutte J, Johnson DS, Bernstein BE, Nusbaum C, Myers RM, Brown M, Li W, Liu S. 2008. Model-based analysis of ChIP-Seq (MACS). *Genome Biol* 9:R137. <https://doi.org/10.1186/gb-2008-9-9-r137>.
  79. Kent WJ, Zweig AS, Barber G, Hinrichs AS, Karolchik D. 2010. BigWig and BigBed: enabling browsing of large distributed datasets. *Bioinformatics* 26:2204–2207. <https://doi.org/10.1093/bioinformatics/btq351>.
  80. Robinson JT, Thorvaldsdóttir H, Winckler W, Guttman M, Lander ES, Getz G, Mesirov JP. 2011. Integrative genomics viewer. *Nat Biotechnol* 29:24–26. <https://doi.org/10.1038/nbt.1754>.
  81. Dallies N, François J, Paquet V. 1998. A new method for quantitative determination of polysaccharides in the yeast cell wall. Application to the cell wall defective mutants of *Saccharomyces cerevisiae*. *Yeast* 14:1297–1306. [https://doi.org/10.1002/\(SICI\)1097-0061\(1998100\)14:14<1297::AID-YEA310>3.0.CO;2-L](https://doi.org/10.1002/(SICI)1097-0061(1998100)14:14<1297::AID-YEA310>3.0.CO;2-L).
  82. Masuko T, Minami A, Iwasaki N, Majima T, Nishimura SI, Lee YC. 2005. Carbohydrate analysis by a phenol-sulfuric acid method in microplate format. *Anal Biochem* 339:69–72. <https://doi.org/10.1016/j.ab.2004.12.001>.
  83. Graham LM, Tsoni SV, Willment JA, Williams DL, Taylor PR, Gordon S, Dennehy K, Brown GD. 2006. Soluble Dectin-1 as a tool to detect beta-glucans. *J Immunol Methods* 314:164–169. <https://doi.org/10.1016/j.jim.2006.05.013>.
  84. Winkelstroter LK, Bom VL, de Castro PA, Ramalho LN, Goldman MH, Brown NA, Rajendran R, Ramage G, Bovier E, Dos Reis TF, Savoldi M, Hagiwara D, Goldman GH. 2015. High osmolarity glycerol response PtcB phosphatase is important for *Aspergillus fumigatus* virulence. *Mol Microbiol* 96:42–54. <https://doi.org/10.1111/mmi.12919>.
  85. Schneider CA, Rasband WS, Eliceiri KW. 2012. NIH Image to ImageJ: 25 years of image analysis. *Nat Methods* 9:671–675. <https://doi.org/10.1038/nmeth.2089>.
  86. Cano LE, Singer-Vermes LM, Vaz CAC, Russo M, Calich VLG. 1995. Pulmonary paracoccidioidomycosis in resistant and susceptible mice: relationship among progression of infection, bronchoalveolar cell activation, cellular immune response, and specific isotype patterns. *Infect Immun* 63:1777–1783. <https://doi.org/10.1128/IAI.63.5.1777-1783.1995>.
  87. Guerra ES, Lee CK, Specht CA, Yadav B, Huang H, Akalin A, Huh JR, Mueller C, Levitz SM. 2017. Central role of IL-23 and IL-17 producing eosinophils as immunomodulatory effector cells in acute pulmonary aspergillosis and allergic asthma. *PLoS Pathog* 13:e1006175. <https://doi.org/10.1371/journal.ppat.1006175>.
  88. Marim FM, Silveira TN, Lima DS, Jr, Zamboni DS. 2010. A method for generation of bone marrow-derived macrophages from cryopreserved mouse bone marrow cells. *PLoS One* 5:e15263. <https://doi.org/10.1371/journal.pone.0015263>.
  89. Mech F, Thywissen A, Guthke R, Brakhage AA, Figge MT. 2011. Automated image analysis of the host-pathogen interaction between phagocytes and *Aspergillus fumigatus*. *PLoS One* 6:e19591. <https://doi.org/10.1371/journal.pone.0019591>.